FUEL CELL-HYBRID ELECTRIC VEHICLE POWER TRAIN SYSTEM DESIGN AND CONTROL

Di Wu

A Thesis

In

The Department

Of

Electrical and Computer Engineering

Presented in Partial Fulfillment of the Requirements

for the Degree of Master of Applied Science at

Concordia University

Montréal, Québec, Canada

August 2008

Your file Votre référence
ISBN: 978-0-494-45355-1
Our file Notre référence
ISBN: 978-0-494-45355-1

ABSTRACT

Fuel Cell-Hybrid Electric Vehicle Power Train System Design and Control

Di Wu

Recently, due to elevated oil prices and the need for low emissions, the automotive industry has been clamoring for cleaner, more energy-efficient vehicles. Fuel cell-hybrid electric vehicles (FC-HEV) are considered to be one of the most promising alternatives, because of their evident advantages of much higher fuel efficiency and lower (or zero) emissions, without any significant restriction on driving range and vehicle performance. However, a number of severe obstacles need to be overcome to attain widespread commercialization of FC-HEVs. The most critical aspects of fuel cell vehicle research include the development of optimal power management strategies and design of efficient power train architectures.

Firstly, this thesis attempts to solve the critical power management problem through the optimal design, modeling, and testing of innovative power control strategies. Thereafter, the advantages and limitations of the proposed strategies are compared and analyzed in depth. Secondly, the thesis also discusses the selection of suitable power train configurations, followed by the power electronic system design, based on hybridization degree and component characteristics. The circuit-level simulation results indicate that the power electronic control system can precisely implement the overall power control strategy, starting from the high-level supervisory control system. Finally, an attractive short-term future option, in the form of a plug-in fuel cell hybrid vehicle (FC-PHEV), is introduced. A suitable power management strategy is designed for the proposed FC-PHEV, with detailed discussions on critical performance as well as practical issues.

ACKNOWLEDGMENTS

The author would like to express her sincere gratitude to her research supervisor, Dr. Sheldon Williamson for his invaluable guidance, advice, friendship, and financial support throughout the course of her Master's program.

The author would like to thank her colleagues in the Power Electronics and Energy Research Group, at the P. D. Ziogas Power Electronics Laboratory, for their helpful discussions and suggestions. In particular, the author would like to express her sincere gratitude towards Dr. Pragasen Pillay, Dr. Luiz Lopes, and Mr. Joseph Woods, for their valuable suggestions and comments, provided during the bi-weekly group meetings.

Last, but not least, the author is very grateful towards her parents, whose constant support made it possible to finish her work successfully.

TABLE OF CONTENTS

LIST OF FIGURES

LIST OF TABLES

LIST OF ACRONYMS

ADVISOR	Advanced Vehicle Simulator
BEV	Battery electric vehicle
CDM	Charge depleting mode
CSM	Charge sustaining mode
DOE	Department of Energy
ECMS	Energy consumption minimization strategy
ESS	Energy storage system, usually a battery
EV	Electric vehicle, also battery-electric vehicle
FCV	Fuel cell vehicle
FCHEV	Fuel cell based hybrid electric vehicle
FC-PHEV	Fuel cell plug-in hybrid electric vehicle
HEV	Hybrid electric vehicle
HWFET	Highway Fuel Economy Test cycle
ICE	Internal combustion engine
IGBT	Insulated-Gate Bipolar Transistor
Li	Lithium
LF	Load follower
MPGe	Miles per gallon equivalent
MPG	Miles per hour
NiMH	Nickel metal hydride
PEM	Proton electrolyte membrane

PHEV	Plug-in hybrid electric vehicles
PM	Permanent magnet
RFC	Regenerative fuel cell
SOC	State of Charge
SRM	Switched reluctance motor
SUV	Sport utility vehicle
UDDS	Urban Dynamometer Driving Schedule cycle
URFC	Unitized regenerative fuel cell

CHAPTER 1

INTRODUCTION

1.1 BACKGROUND

Stimulated by global attention as well as stringent regulations on emissions and fuel economy, global warming, and constraints on energy resources, electric, hybrid electric, and fuel cell vehicles are receiving extensive interest from research programs and automakers alike. The transportation sector consumes almost two-thirds of petroleum in North America alone. With the rapid economic growth of China, India, and other developing countries, road vehicles are projected to be 5 times larger in the next 15-20 years' time [1]. But petroleum is a finite resource and gasoline will probably become a very expensive energy source in the future. Also, the consumption of hydrocarbon fuels releases carbon dioxide into the atmosphere. Carbon dioxide is the major greenhouse gas, raising concerns with regards to global warming. Therefore, adopting advanced automotive propulsion technologies that improve energy usage efficiency and reduce transportation's impact on global warming can have a significant impact on future quality of life.

1.1.1 HYBRID ELECTRIC VEHICLE (HEV) ARCHITECTURE

Compared to conventional vehicles, hybrid electric vehicles are more fuel efficient since they combine the advantage of an electric motor drive and the existing internal combustion engine (ICE) to propel the vehicle. With this arrangement, the ICE operation

can be optimized and regenerative braking energy can be recovered, thereby significantly increasing the overall vehicle efficiency [2]. The HEV power train can be divided into 3 categories based on their configurations: series hybrids, parallel hybrids, and parallel-series combined hybrids, as shown in Fig. 1-1.

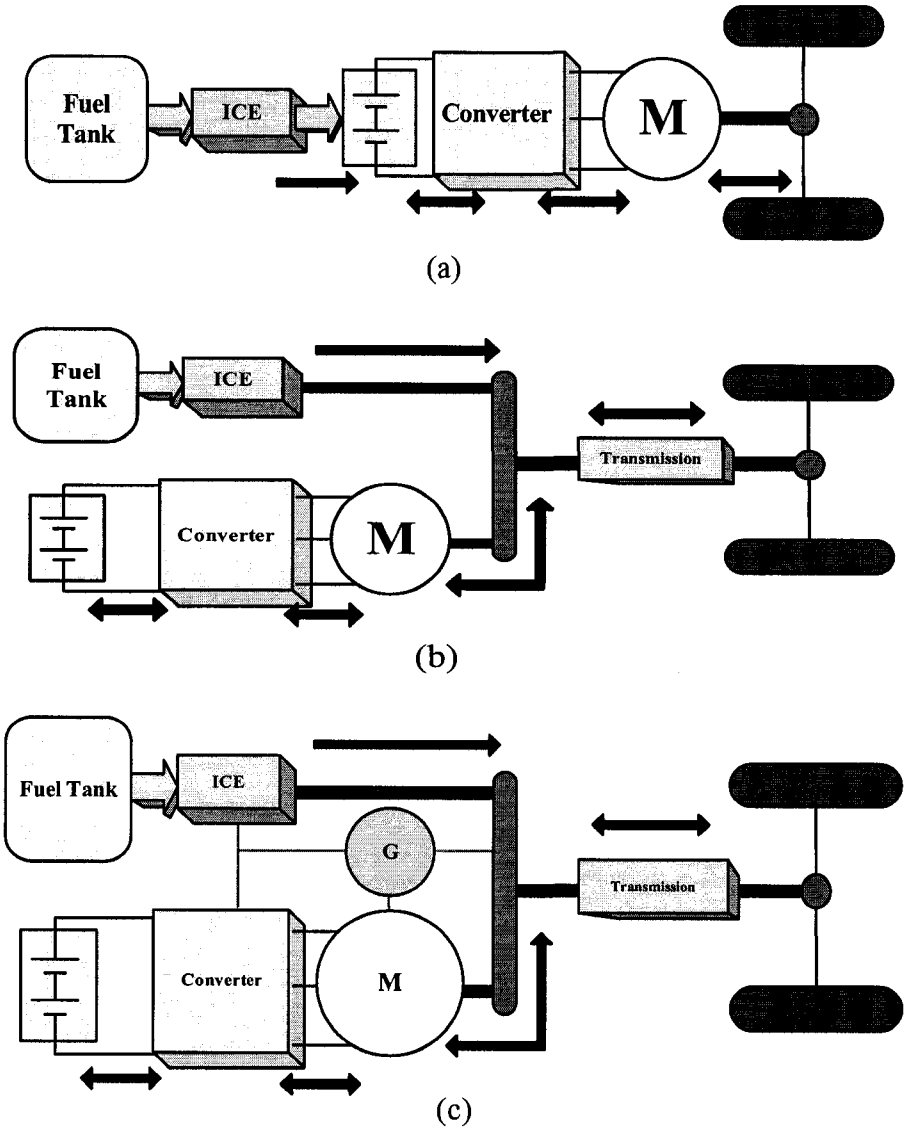

Fig. 1-1 (a) Series (b) Parallel and (c) Series-parallel combined HEV drive trains

The series hybrid is the simplest HEV topology. The electric motor, which is mechanically attached to the drive train, represents the only power source to drive the

vehicle. The mechanical power output from the ICE is first converted into electric power, using an alternator. The converted power either charges the on-board battery system or bypasses the battery to propel the wheels through the same electric motor and mechanical transmission. Conceptually, it is an engine-assisted electric vehicle (EV), which aims to extend the overall driving range. Due of the absence of clutches throughout the mechanical link, the series HEV has a definite advantage of flexibility to locate the engine-generator set [3]. Although the series HEV has the added advantage of drive train simplicity, it requires 3 machines; the engine, the generator, and the electric motor, and thereby, the overall efficiency is found to be relatively low. An additional disadvantage of series HEVs is that the 3 machines need to be sized for maximum continuous power, in order that the vehicle can successfully climb up a steep grade.

As opposed to the series HEV architecture, the parallel HEV allows both the ICE and the electric motor to deliver power to drive the wheels. Since both the ICE and electric motor are generally coupled to the drive shaft of the wheels through clutches, the propulsion power may be supplied by the ICE alone, by the electric motor alone, or by both. Thus, conceptually, a parallel HEV architecture is inherently an electric-assisted vehicle, designed to achieve lower emissions and fuel consumption. The electric motor can be used as a generator to charge the battery through regenerative braking or absorb power from the ICE when its output is greater than that required to drive the wheels. A distinct advantage over the series HEV architecture is that the parallel HEV needs only 2 propulsion devices; the ICE and the electric motor [2]. Therefore, the parallel HEV topology easily surpasses the series HEV topology in terms of energy efficiency. This is mainly because most of the ICE power need not be converted into electrical energy,

before being delivered to the wheel. Another obvious advantage of the parallel HEV drive train is that a smaller ICE and a smaller electric motor can be used to get the same performance, until the battery is depleted. However, in such an arrangement, regenerative braking will be less efficient due to efficiency loss in the transmission system.

A series-parallel HEV architecture incorporates the characteristics of both the series and parallel systems by using a power split device between the motor, generator, and the ICE, as shown in Fig. 1-1 (c). Although possessing the advantageous features of both the series and parallel HEVs, the series-parallel HEV is relatively more complicated and costly, and a more intricate power control strategy is needed.

1.1.2 Plug-in Hybrid Electric Vehicle (PHEV) Architecture

Recently, much of the automotive industry's research has been focused on Plug-in hybrid electric vehicles (PHEVs). PHEVs are hybrid electric vehicles that can draw and store energy from an electric grid (or a renewable energy source), to eventually propel the vehicle. The architecture of a typical PHEV is shown in Fig. 1-2.

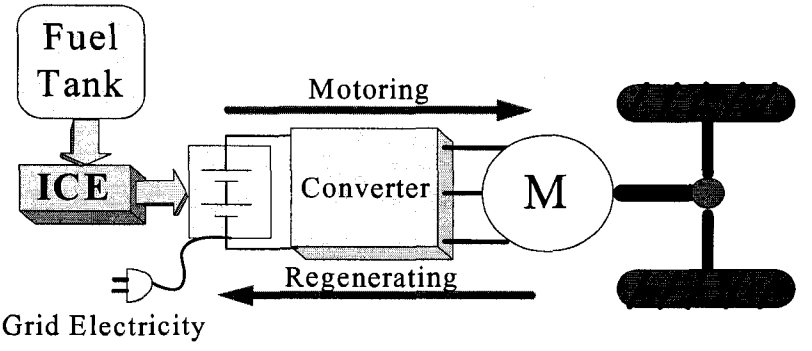

Fig. 1-2 Typical plug-in HEV drive train configuration

This simple functional change allows a PHEV to displace petroleum with multi-source electrical energy, including renewable energy resources, such as wind and

solar energy. Such a change has critical beneficial impacts on the overall transportation sector petroleum consumption, total emissions, as well as on the performance and makeup of the electrical grid. PHEVs are seen as one of the most promising means to improve the near-term sustainability of the transportation as well as stationary energy sectors. Surveys have shown that there exists a considerable market for PHEVs. *Renault* and *Daimler-Chrysler* have produced limited production PHEVs. *General Motors* and *Ford Motor Co.* have recently developed and displayed PHEV concept vehicles [4].

1.1.3 Fuel Cell-Hybrid Electric Vehicle (FC-HEV) Architecture

In the long term scenario, fuel cells represent one of the most appealing technologies for vehicle propulsion to further achieve high fuel efficiency, zero emissions, and low noise. Fuel cells are considered among the most promising alternative power sources, which can replace the conventional internal combustion engine (ICE). Compared to battery-powered electric vehicles (EVs), fuel cell vehicles (FCVs) have the advantage of longer driving range without a long battery charging time. In addition, compared to ICE vehicles, FCVs also depict comparatively higher energy efficiency and much lower emissions, due to direct conversion of free energy from the fuel into electric energy, without undergoing combustion. However, to fully achieve the potential energy savings of a fuel cell vehicle, it is important to recover the braking energy and ensure the operation of the FC system at maximum efficiency over the entire range of driving conditions encountered. This can be reached by a hybridization approach similar to gasoline-engine powered HEV. Furthermore, FC-HEVs present the advantages of cleaner and more efficient energy source, combined with the energy savings typical of EVs.

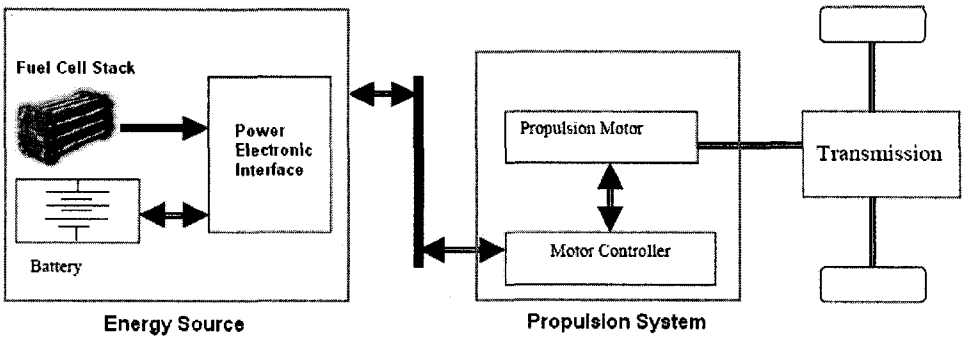

Fig. 1-3 Typical power train layout of FCHEV

A typical power train of a fuel cell vehicle is as shown in Fig. 1-3. While most major automotive companies are investing in fuel cell vehicles, many challenges remain in getting fuel cell vehicles in the market. The major challenges include increasing fuel cell reliability, developing hydrogen infrastructure, improving on-board hydrogen storage capabilities, and overall cost reduction. One of the main research focuses is to develop a power control strategy and a power management system, which includes a fuel cell system, an energy storage system (ESS), and a suitable power electronic interface. Investigation of these problems will be the main focus of this thesis.

1.2 OPERATING PRINCIPLE OF A FUEL CELL

The application of fuel cells in vehicles has been the focus of auto manufacturers in recent decades. In contrast to a chemical battery, the fuel cell generates electric energy rather than storing it, and continues to do so, as long a fuel supply is maintained. Today, the following 5 types of fuel cells are currently being developed: the alkaline fuel cell (AFC), the proton exchange membrane fuel cell (PEM), the phosphoric acid fuel cell (PAFC), the molten carbonate fuel cell (MCFC), and the solid oxide fuel cell (SOFC) [5]. The 5 types of fuel cells differ in terms of efficiency, operating temperatures, and input

fuel requirements. Compared to other types of fuel cells, the PEM fuel cell is considered to be a prime candidate for use in automotive applications due to its higher power density (power per fuel cell active area) and lower operating temperature (around 80°C) as well as faster start-up time (less than 1 minute).

The basic operation of a PEM fuel cell is shown in Fig. 1-4 [7]. PEM fuel cells produce electricity via cell reactions, from the chemical energy stored in the fuel source. Separate gas flow channels provide for continuous fuel flow (typically hydrogen) to the anode and continuous oxidant flow (typically air) to the cathode. For automotive applications, hydrogen is provided either directly from on-board storage (direct hydrogen) or by onboard reforming of a hydrogen-bearing fuel. An electrolyte membrane separates the 2 electrodes. The products of the cell reaction are water, electrical power (electric current with a corresponding voltage), and thermal energy. Several cells are normally connected in series or parallel to form a fuel cell stack, in order to produce sufficient voltage for many practical applications.

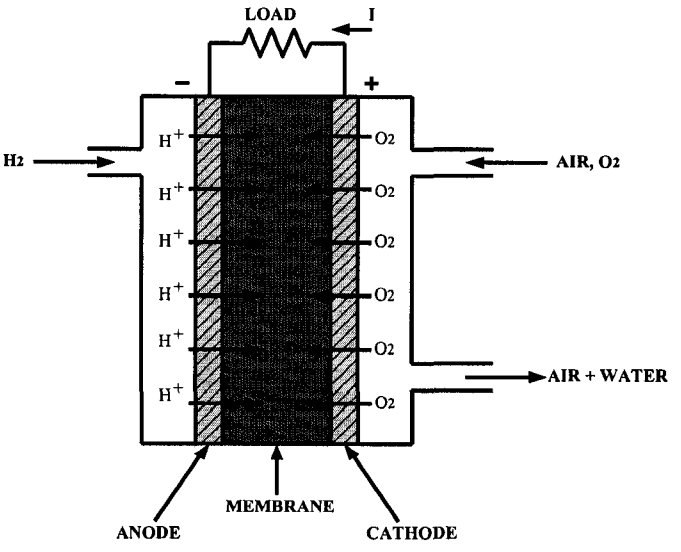

Fig. 1-4 Principle of operation of PEM fuel cells [7]

The polarization curve is the most important characteristic of any fuel cell. Fig. 1-5 to Fig. 1-7 [5], [6] illustrates typical fuel cell polarization curves.

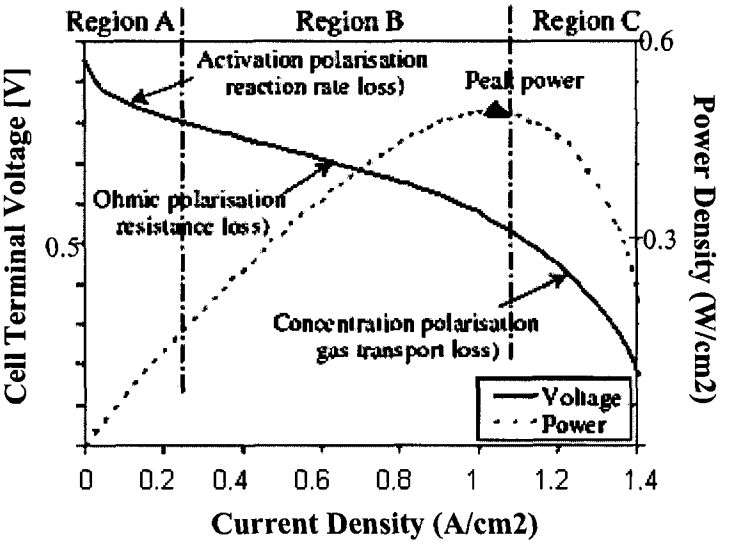

Fig. 1-5 Typical fuel cell stack I-V and power curve [5]

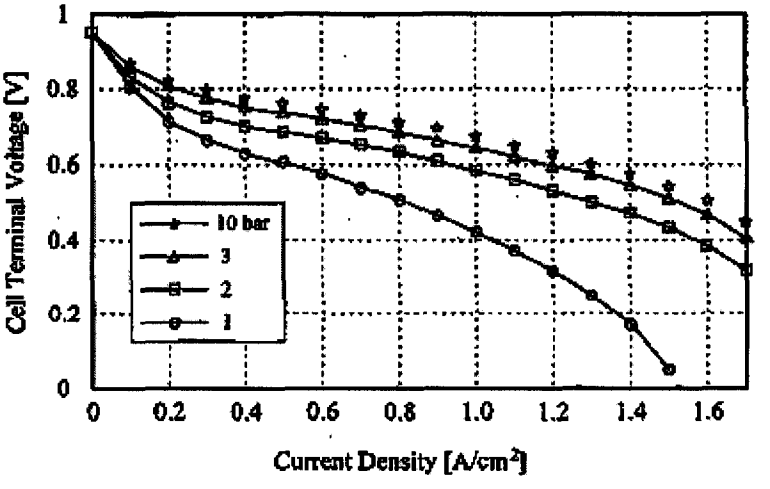

Fig. 1-6 Typical fuel cell polarization characteristics at stack pressure of [1, 2, 3, 10] bar at T=80°C [6]

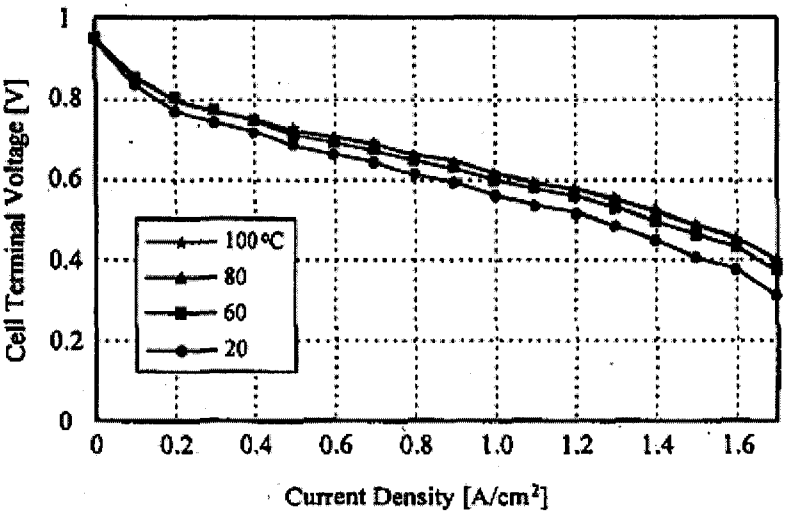

Fig. 1-7 Typical fuel cell polarization characteristics at varying temperatures at P=3 bar

It can be noticed, that for a given current density, increasing cathode pressure or increasing fuel cell operating temperature, generally results in higher voltage, higher power density, and higher energy efficiency. Also, for a given set of conditions, voltage decreases with increasing current density. Furthermore, the power produced increases with increasing current density, until a current density is reached, at which maximum power output occurs.

1.3 POWER MANAGEMENT PROBLEM OF FC-HEVS

The benefits of hybridization of a fuel cell vehicle with an energy storage system (ESS), such as batteries, can be summarized as follows:

- Reduce the size of the FC, which is the most expensive component of the system;
- Increase the flexibility to optimize the combination of component characteristics and energy management strategy, in order to compensate the impacts of slow response of the fuel cell system, and improve the system efficiency;
- Solve the cold start-up problem of the fuel cell system, by using on-board energy

storage; and recover braking energy, which is produced and made available in the form of electricity.

A FCHEV is an integrated system that consists of many sub-systems, such as fuel cell system, motor system, battery, brakes, etc., as shown in Fig. 1-8. Each sub-system is a complex device that has its own functionality and desired performance, and almost every sub-system is equipped with sensors, actuators, and a control system, to regulate its behavior. Moreover, all sub-systems need to be coordinated in an optimal manner to achieve different objectives such as fuel economy, power components efficiency, and drivability. Therefore, a system level supervisory power train controller is required to accomplish this vital task.

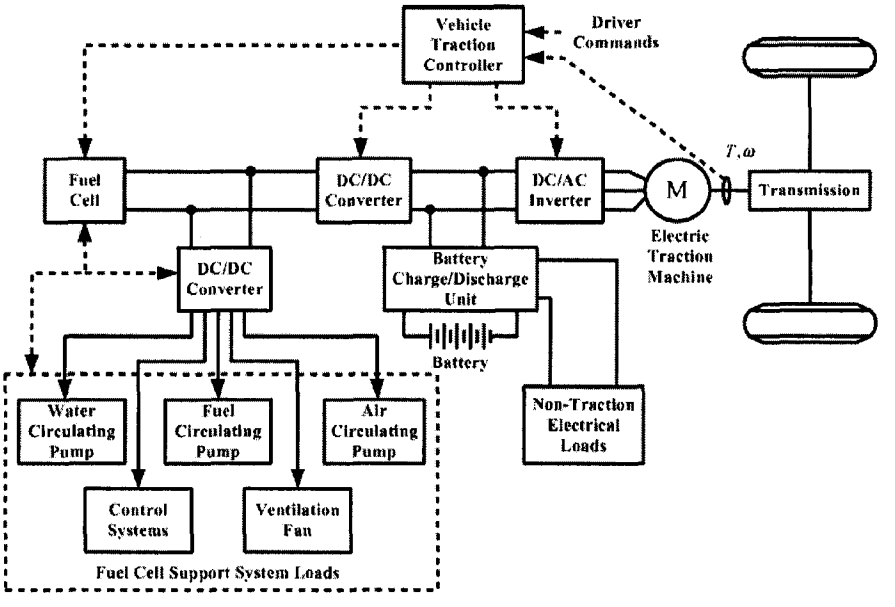

Fig. 1-8 Schematic of a fuel cell based power system for a passenger car

In this thesis, one of the main focal points includes the vehicle power train system-level control. Generally, a power train control system can use 2-level hierarchical control architecture, as illustrated in Fig. 1-9.

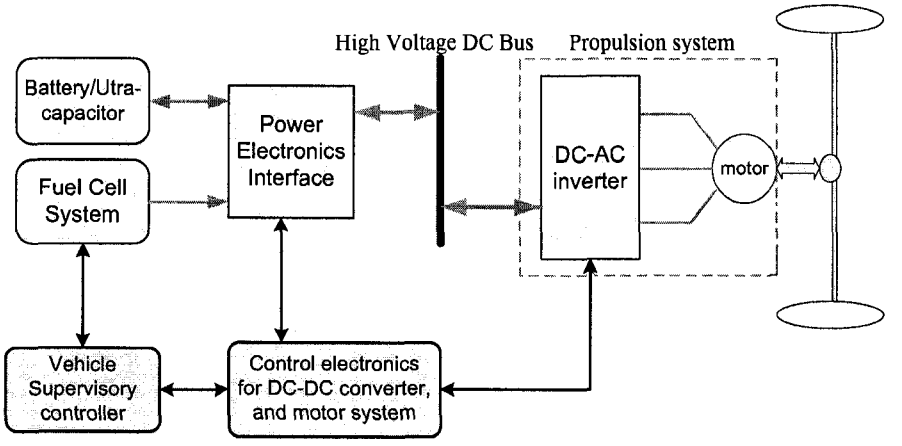

Fig. 1-9 Power train control system of a FCHEV

The vehicle supervisory controller collects the data from fuel cell, battery, and motor system, and generates an optimized power distribution, based on a designed power control strategy. Meanwhile, the circuit-level control electronics for DC/DC converters, inverter, and motor provide feedback control, according to the reference power value (usually transfer to reference current) from the high-level supervisory controller. In other words, the major task of the high-level controller is to solve the power distribution problem, in order to improve fuel economy, component efficiency, and vehicle performance; while the main task of the low-level control system can be treated as a typical regulating or tracking control problem.

1.4 THESIS OBJECTIVE

The primary objective of this thesis is to find the most suitable power train configuration and control scheme for fuel cell-hybrid electric vehicles (FC-HEVs). The thesis seeks to determine: the optimal connection scheme between the fuel cell system and the battery, interaction between the 2 power sources, and management of overall

power distribution. In order to achieve these goals, 2 types of power control strategies are designed for an FC-HEV. Thereafter, their performance characteristics are comparatively studied. In addition, the FC-HEV power train configurations are designed and selected by considering the power component characteristics as well as cost and sizing issues.

Finally, this thesis also proposes the potential of a fuel cell plug-in hybrid vehicle (FC-PHEV) as a transition from FC-HEVs. A new power train configuration and power control strategy is designed for the proposed FC-PHEV. In the thesis, the system level vehicle modeling, control strategy design, and performance studies are conducted in the Advanced Vehicle Simulator (ADVISOR) software, which is based on Matlab/Simulink environment. For circuit-level modeling and system interface, the PowerSim (PSIM) software is used.

1.5 THESIS OUTLINE

The contents of this thesis are organized into 6 chapters. Chapter 1 provides a background of hybrid electric vehicle development, followed by an introduction to fuel cell technology and fuel cell based hybrid electric vehicle. Chapter 2 introduces system-level modeling of the vehicle baseline and power components in ADVISOR. Chapter 3 initially reviews possible power control strategies for FC-HEVs, and then explains the design and modeling of 2 selected strategies, followed by the simulation-based performance analysis.

Chapter 4 introduces the various FC-HEV power train configurations as well as power converter interfaces and designs. Thereafter, 2 favourable types of power train topologies are chosen based on the hybridization degree, for a mid-size hybrid SUV. The power electronic control systems for each topology are designed for optimal power

regulation and are validated through extensive test conditions. Chapter 5 proposes an innovative fuel cell vehicle option, in the form of a plug-in fuel cell-hybrid electric vehicle. A suitable power management strategy is designed for the proposed FC-PHEV, and the vehicle performance is discussed based on simulation tests. Chapter 6 summarizes the overall research performed in this thesis, by presenting the critical inferences drawn from the studies. Finally, the thesis suggests possible future directions in terms of advanced electric and hybrid electric vehicle research.

CHAPTER 2

FUEL CELL-HYBRID ELECTRIC VEHICLE MODELING

2.1 MODELING ENVIRONMENT

The baseline vehicle and control strategy is modeled and analyzed in the Advanced Vehicle Simulator (ADVISOR) software, which is developed in the MATLAB/Simulink environment [8]. ADVISOR is composed of a group of models, experimentally verified data, and script files. It not only allows the designer to obtain a quick analysis of the performance and fuel economy of conventional, electric, hybrid electric, and fuel cell vehicles, but it also provides detailed simulations and analysis of user-defined power train components, by taking advantage of the modeling flexibility of Simulink and the analytical power of Matlab [9].

ADVISOR uses 3 primary graphical user interface (GUI) screens to guide the user through the simulation process. The GUI facilitates interaction with the raw input and output data that is present in the MATLAB workspace. The vehicle model is depicted graphically using Simulink block diagrams, to define the connections between components, as shown in Fig. 2-1. The component models can be inserted into a vehicle model and then connected to define the flow of torque or speed and power from one component to the next. The arrows entering the top input of a component block in the fuel cell vehicle model, shown in Fig. 2-1, represent a torque and speed or a power demand from one component to the next upstream component. The power demand is based on the vehicle speed requirements and the losses of each component. Arrows entering the

bottom input port of each block represent what the upstream component is able to achieve.

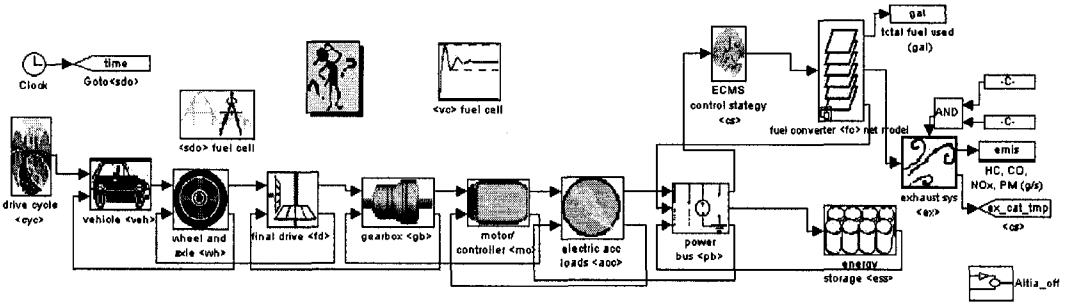

Fig. 2-1 Overall vehicle Simulink diagram in ADVISOR

In general, individual component models are a combination of algorithms programmed in Simulink and data files that store various tuning parameters for the algorithms. By incorporating various vehicle performance and control information into a modular environment within Matlab and Simulink, ADVISOR allows the user to interchange and design a variety of components, vehicle configurations, and control strategies. It also allows quick analysis of the vehicle performance, emissions, and fuel economy of conventional, electric, and hybrid electric vehicles.

2.2 MODELING AND SELECTION OF POWER COMPONENTS

In this section, the sizing and modeling of the FC-HEV power train system are introduced. The power components mainly include the fuel cell system, battery system, and the motor-controller system.

2.2.1 FUEL CELL SYSTEM

As aforementioned, fuel cells are electrochemical devices that convert the energy of a chemical reaction between hydrogen and oxygen directly into electrical energy.

Various types of fuel cells exist, but as stated in chapter 1, the PEM fuel cell is regarded as the most promising option for automotive application, due to its high power density, low operating temperature of about 80°C, and high overall efficiency [10].

ADVISOR includes 2 options for modeling the fuel cell. The first one is based on look-up tables, indexed to the polarization curves, which characterize the fuel cell stack performance. The key assumption is that the system can provide a specific net power, while consuming a set amount of fuel, regardless of how complex the system may be [9]. A used net power vs. efficiency data for PEM fuel cell stack built in ADVISOR is shown in Fig. 2-2.

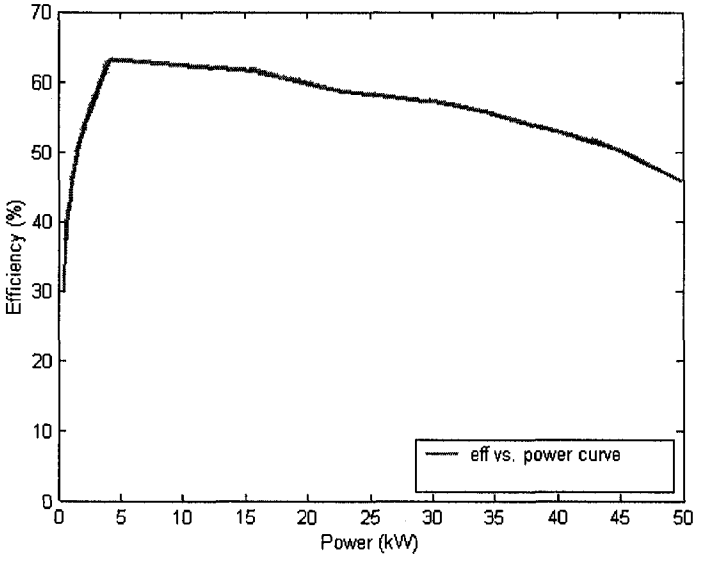

Fig. 2-2 Net power vs. efficiency map for a 50kW fuel cell system model

The performance of the auxiliary systems, such as air compressor and fuel pump, can be also characterized with polarization curves, from experimental data in ADVISOR. The power delivered by the fuel cell system is the difference between the power produced by the fuel cell stack and the power consumed by the auxiliary system. The second option is to model a fuel cell stack in a much more complete manner through a co-simulation

link between ADVISOR and General Computational Toolkit (GCtool). In such a case, the electrochemistry, thermal characteristics, and mass transfer characteristics can also be incorporated. It must be pointed out, though, that such a detailed model is not necessary for overall vehicle system-level performance analysis.

2.2.2 BATTERY SYSTEM

A suitable energy storage system (ESS) is required to assist the fuel cell system, to meet the power demand from the drive train. Currently, lead-acid batteries are employed in conventional cars, because of their low price and rugged structure. On the other hand, for recent HEV applications, nickel metal-hydride (Ni-MH) batteries are commercially used in the market. Compared to lead-acid batteries, Ni-MH batteries generally have much longer lifespan, higher power output, and increased charge and discharge efficiency. Besides, they are also safely recyclable [11]. Ni-MH batteries have been employed successfully in vehicles in the state of California, and demonstrated promise to meet the power and endurance requirements for electric vehicle (EV) propulsion. Meanwhile, Lithium-ion (Li-ion) batteries are likely to become serious competition for Ni-MH in EV/HV applications, but their operating life is still limited. In addition, ultra-capacitors are also currently under investigation in several research programs, but their energy density is much lower than those of batteries. The main advantage of ultra-capacitors is their high power density, which make them great options for hybridizing with battery systems, for supplying short bursts of power during acceleration, or receiving short bursts of regenerative currents, during quick decelerations. Fig. 2-4 shows the energy and power densities comparison of common energy sources [11].

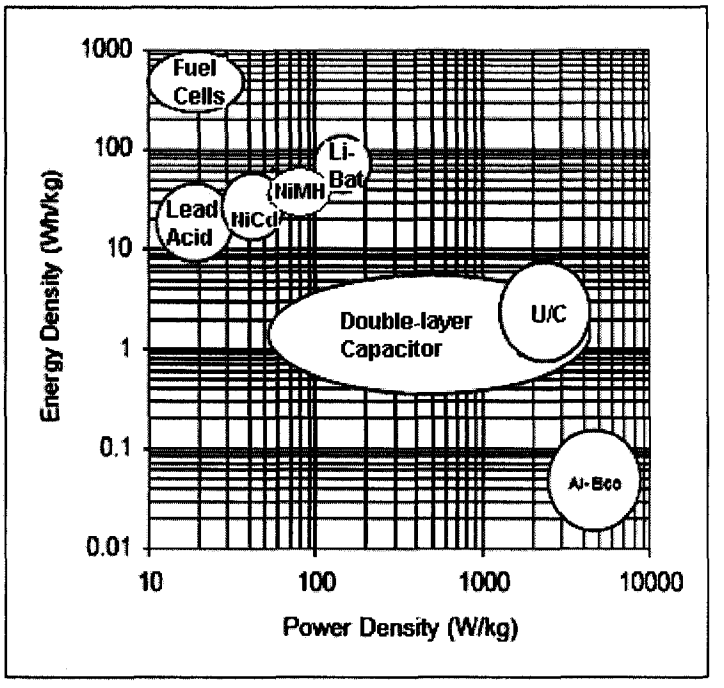

Fig. 2-4 Energy and power densities of various energy storage components [11]

The battery model type used for the FC-HEV under study is the *Ovonic* 45Ah Ni-MH battery. The main performance characteristics of this battery are summarized in Table 2-1. The battery is modeled in ADVISOR based on the internal resistance model, as shown in Fig. 2-5. The circuit determines the output voltage and current based on the load, while estimating the rate at which this power level depletes the resistor through the internal model calculation.

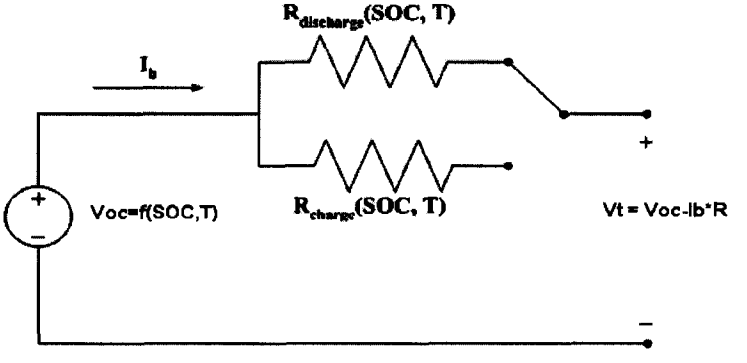

Fig. 2-5 Internal resistance battery model electrical schematic

Due to the non-linear behavior of batteries, the parameters of the simulation circuit are determined from experimental data collected by the Battery Thermal Management Laboratory, manufacturer data sheets, as well as lab tests [12]. At each time step, the net battery current is then used to estimate the change in State of Charge (SOC) of the battery. Fig. 2-6 shows the internal resistance of the battery at 40°C.

Table 2-1 Ni-MH Battery parameters

Nominal Voltage	12 V
Nominal Capacity (C/3)	45 Ah
Nominal Energy (C/3)	598 Wh
Peak Power (10s pulse @ 50%DOD @ 35 deg. C)	3.3 kW
Weight	8 kg
Volume (modules only)	3.2 L

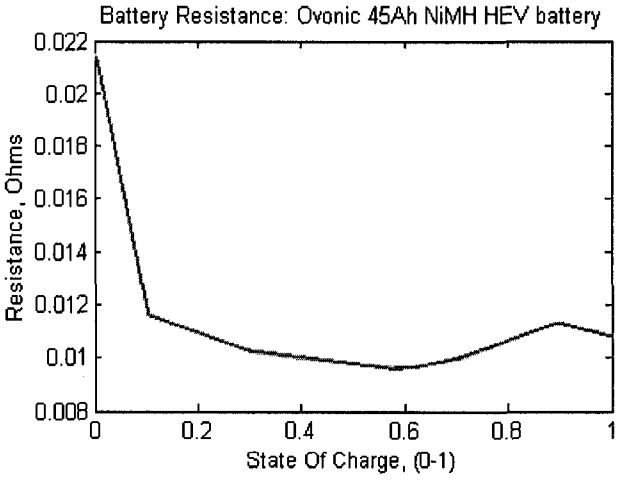

Fig. 2-6 Resistance of the Ni-MH battery at 40 deg. C in ADVISOR

2.2.3 MOTOR-CONTROLLER SYSTEM

The electric traction motor system plays an important role in the performance of a FC-HEV. The main requirements for motor selection include: high torque density and power density; wide speed range, including constant torque and constant power operations; high efficiency over wide speed range, high reliability, and robustness; a reasonable cost [3]. There are 3 motor types suitable for HEV applications: permanent magnet motors, induction motors, and switched reluctance motors. The permanent magnet machines possess high efficiency, high torque, and high power density. However, they inherently have a short constant power range, due to limited field weakening capability. In addition, the back EMF can also be a problem at high speeds, because the inverter must be able to withstand the maximum back EMF generated by the stator winding. The switched reluctance motor (SRM) is a promising candidate for HEVs, due to of its simple construction, simple control, and good extended speed performance. However, since the SRM is not yet widely produced as a standard motor in the market, the overall electric propulsion system cost may be higher than other motor options.

Thus, the popular induction motor (IM) is selected for FC-HEV modeling in the thesis due to its simplicity, robustness, and adequate extended speed range. Also, IMs do not have back EMF to deal with, at high speeds [3]. Field-oriented control makes an IM behave like a simple DC machine. In ADVISOR, the entire motor system is modeled based on motor efficiency maps, where the motor efficiency is determined as a function of toque and speed. Fig. 2-7 shows the efficiency map of the *Westinghouse* 75kW IM. The bold lines represent the maximum torques, according to the speed of the motor.

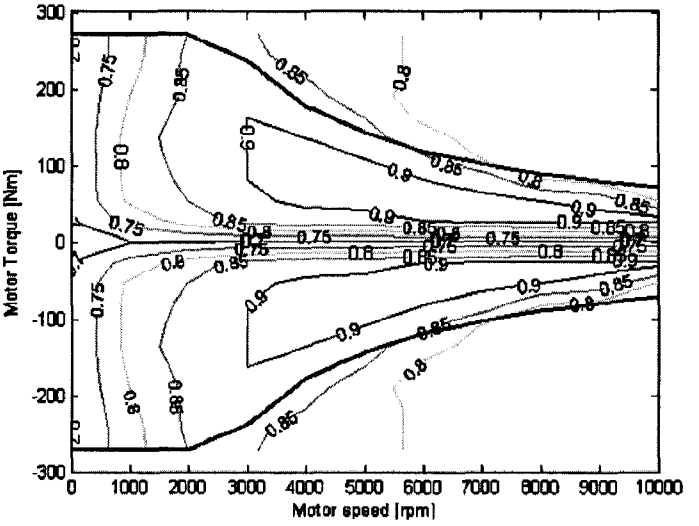

Fig. 2-7 Efficiency map of a *Westinghouse* 75kW AC induction motor [8]

Corresponding to the backward-facing vehicle modeling approach, the desired speed and torque requests, propagated from the transmission, are translated by the motor model into a power request through a series of mathematical equations.

2.2.4 BASELINE VEHICLE

The vehicle dynamic model is described by the typical force balance equation as shown in 2-1, from which the total driving force is computed as the sum of rolling resistance force, aerodynamic resistance force, acceleration force, and climbing resistance force. The model first calculates the required driving force, according to the required acceleration. Thereafter, the achievable acceleration is calculated, based on the output driving force. The vehicle speed is determined by the driving cycle, transmission gear ratio, and the wheel radius. In this thesis, we assume that the vehicle has a one-speed transmission.

$$F_{total} = F_{rolling} + F_{aero} + F_{acc} + F_{climb} \qquad (2\text{-}1)$$

The vehicle characteristics are assumed to be based on current production of baseline conventional vehicles. The vehicle parameters are selected based on 2 types of vehicles: the mid-size family sedan and mid-size SUV. Table 2-2 outlines the vehicle modeling assumptions.

Table 2-2 Vehicle specifications

Vehicle Type	Mid-size SUV	Mid-size Sedan
HEV glider mass	1179 kg	636 kg
Cargo Mass	136 kg	136 kg
Fuel Cell Vehicle Goss Mass	2095 kg	1300 kg
Rolling Resistance	0.012	0.012
Frontal Area	$2.66m^2$	$2.0\ m^2$
Coefficient of Drag	0.44	0.35

2.3 SUMMARY

This chapter summarized the sizing and modeling aspects of the vehicle and its main power components. The ADVISOR software as a modeling and simulation environment was introduced. The complete modeled block diagram of the FC-HEV is shown in Fig. 2-8.

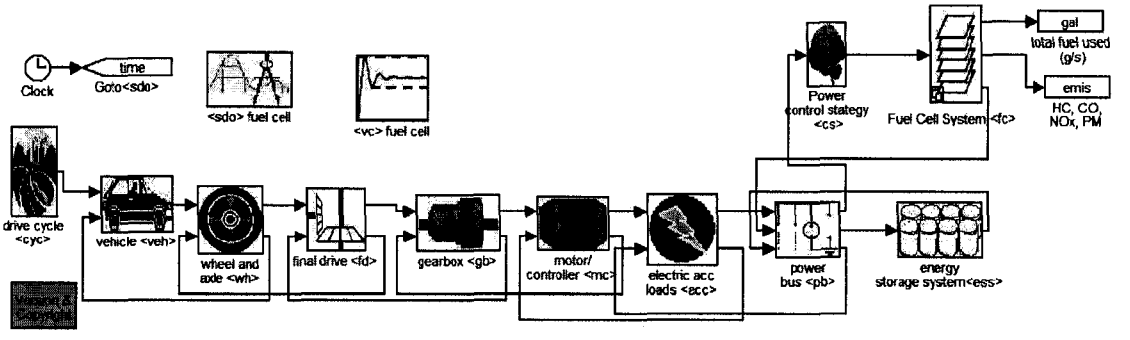

Fig. 2-8 Block diagram of the modeled FC-HEV drive train

As mentioned earlier, the PEM fuel cell is used due to its high power density, low operating temperature, and high efficiency. For system level performance analysis, the fuel cell system is modeled by look-up tables, indexed to the polarization curves, which characterize the fuel cell stack performance. The nickel metal-hydride (Ni-MH) battery is used as the ESS, because of its high energy density and reasonable cost. The battery is modeled based on the internal resistance model and experimental data. The motor system used is an AC induction motor, which is modeled based on its efficiency map. The baseline vehicle parameters are selected based on current production of conventional vehicles. In the analyses performed in the ensuing chapters, 2 types of baseline vehicles are considered; they include a mid-size family sedan and a mid-size sports utility vehicle (SUV).

CHAPTER 3

POWER CONTROL STRATEGIES FOR FC-HEVS

3.1 INTRODUCTION

A typical drive train layout of a FC-HEV with control information flow and power flow is shown in Fig. 3-1. The FC-HEV utilizes the fuel cell system as the main power source to provide electricity and uses a reversible energy storage accumulator, such as a battery or an ultra capacitor, as a supplementary power source. This hybridization not only downsizes the fuel cell and fulfills transient power demand fluctuation, but also leads to significant energy savings through regenerative braking energy recovery [13].

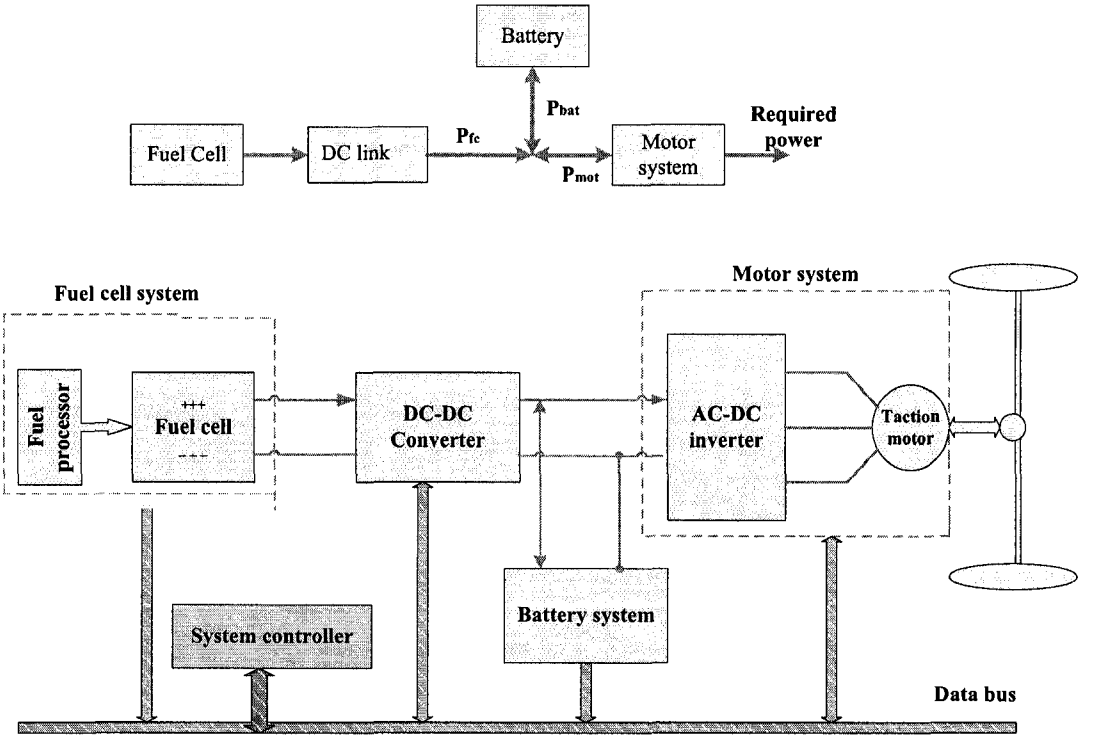

Fig. 3-1 Main schematic of the overall system

As is the case with regular hybrid electric vehicles (HEVs), a good system level power control strategy is essentially required to solve the problem of managing the power sharing between the fuel cell and the battery. An optimal control strategy design helps achieve maximum fuel economy, system efficiency, and maximize ESS life span, while maintaining required vehicle dynamic performance. In addition, simplicity, feasibility, and robustness are also important factors to evaluate different power control strategies. Various types of power control strategies have been proposed for HEVs, which could be extended to FC-HEV applications [14]-[22].

Some of the popular FC-HEV power control strategies are reviewed in the ensuing sections. Thereafter, optimized design, modeling, and in-depth analysis are performed on 2 types of control strategies, namely the load follower control scheme and the equivalent consumption minimization strategy (ECMS). In order to investigate their control performance, and to further optimize their respective designs, detailed comparisons and analyses based on simulation tests, are also presented in this chapter.

3.2 Review of FC-HEV Power Control Strategies

The general goal of the power control strategy for a typical FC-HEV drive train is to maximize the vehicle system efficiency and enhance fuel economy, while maintaining the required vehicle performance. There are several global optimization algorithms, such as dynamic programming (DP), developed for HEVs, to find the optimal solution of power distribution [21]. The DP method is a cost function based dynamic optimization tool, which can guarantee global optimal solution up to the grid accuracy of the states. However, these kinds of strategies are based on a prior knowledge of future driving conditions. Therefore, they are not suitable for real-time control, but they can best serve

as a benchmark for improving other control strategies.

Rule-based control strategies are popular for FC-HEV power management, due to their simplicity and feasible implementation. These types mainly include the thermostat scheme [8], load follower scheme [8], [14], and fuzzy logic scheme [16]-[18]. The thermostat scheme features simplicity and robustness. Under this scheme, the fuel cell will turn on and off based on the battery SOC. The fuel cell turns on when the SOC reaches the low limit and turns off when the SOC reaches the high limit. When the fuel cell is on, it will always operate at the most efficient power level, as shown in Fig. 3-2, which compares the fuel cell operating point of the thermostat scheme with load follower scheme. Although this strategy is simple and easy to control, it has some disadvantages; firstly, it cannot satisfy vehicle driving requirements, especially during acceleration or high power command. Moreover, this strategy leads to frequent charging/discharging of the battery, which is unfavorable.

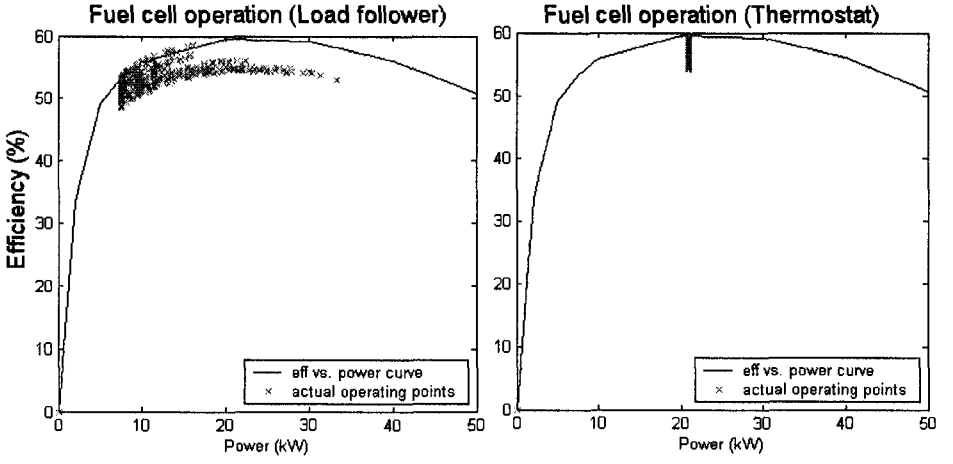

Fig. 3-2 Fuel cell operating points with the load follower and the thermostat scheme

The load follower scheme, to a large extent, can solve the problems occurring in the thermostat scheme. The basis of the power follower scheme is to determine the

operation state of the fuel cell, according to the power demand from the vehicle and the battery state of charge (SOC). The fuel cell output is never to be a constant value, but tends to change, following the transient power requirements in a reasonable region. A minimum and a maximum output power level (Pfc_min, Pfc_max) should be determined to avoid the fuel cell system operating in low efficiency. Meanwhile, the battery SOC should be controlled within a range where regenerative braking energy can be effectively absorbed, while ensuring battery life. In this thesis, this control strategy is selected for the purpose of optimal design and simulation test based analyses in the ensuing sections, because it can achieve better control performance compared to thermostat, and it is easy to create an acceptable design within a short time.

More recently, fuzzy logic is becoming increasingly popular in hybrid vehicle control, because it enables the development of dynamic rule-based behavior. It solves the problem that exists in static control approaches, where the parameters are normally optimal for a specific vehicle type and a specific driving condition, while becoming sub-optimal in other conditions. The main advantage of fuzzy logic control schemes is that they can be tuned and adapted to the specific driving conditions and plant dynamics, thus enhancing the degree of freedom of control [18]. Another benefit is that it does not depend on accurate mathematical modeling, which is hard to obtain for complex systems, such as FC-HEVs.

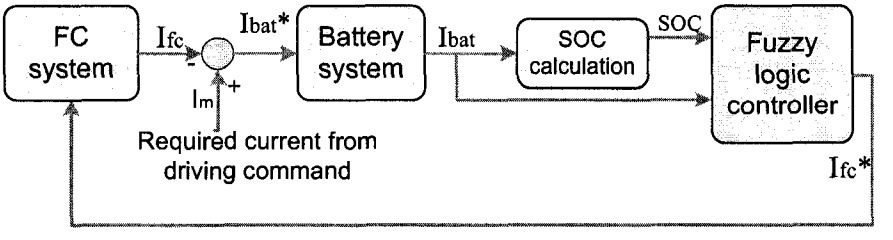

Fig. 3-3 Fuzzy logic based power control scheme

In a fuzzy logic controller, the knowledge of an expert can be coded in the form a rule-base, and can be used in decision making. A basic type of fuzzy logic based power control scheme is illustrated in Fig. 3-3 [16]. As is clear, the inputs of the fuzzy controller are battery SOC and battery current, and the fuzzy output is the required current for the fuel cell. Fig. 3-4 shows the basic analysis method for fuzzy logic control. The fuzzifier converts the crisp input value into a fuzzy value, with degrees of membership functions.

The inference engine combines the fuzzy rules into a definite map, from a fuzzy set of inputs to the output, based on fuzzy logic principles. The defuzzifier then reconverts the resulting fuzzy value into a specific crisp value, as a reference variable. The heart of a fuzzy system is a set of knowledge-based IF-THEN fuzzy rules. However, the main limitation of a fuzzy logic control strategy is its complexity, which limits implementation flexibility.

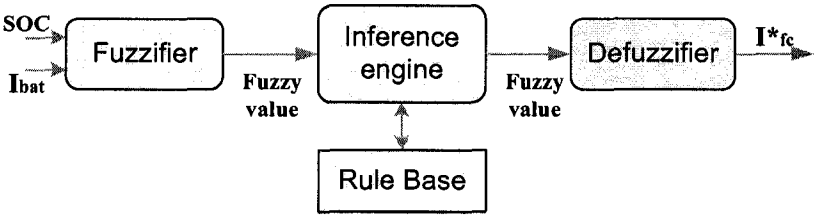

Fig. 3-4 Structure of fuzzy logic controller

To develop a cost function based optimal algorithm, which is real-time applicable, some improved strategies have been proposed. The Stochastic Dynamic Programming (SDP) has been proposed to solve the power management as a stochastic problem [22]. The basic principle of SDP problem formulation is to model the power command as a stochastic process, and an optimal controller based on the stochastic model can be designed, in order to find an optimal control policy that maps the control decision against the vehicle operation states. At the same time, the disadvantage is that it is

computationally expensive to build cost tables and corresponding optimal control for complex dynamic systems. Another popular cost function based control strategy is the equivalent consumption minimization strategy (ECMS) [19], which is developed for parallel HEVs. The ECMS replaces the global cost function to a local one, which adjusts the instantaneous power split by calculating an equivalent fuel cost function for an array of power splits between 2 energy sources, and selects the split with the lowest fuel cost. This type of control strategy can often reach a nearly optimal operation set point. The ECMS strategy, as a representative of cost-function based control strategies, is selected for optimized design and simulation-based study in the ensuing sections.

3.3 Design and Performance Analysis of Power Control Strategies

3.3.1 Load Follower Strategy

The power/load follower scheme is primarily a rule-based control scheme, which determines the operation state of the fuel cell, according to the power demand from the vehicle and the battery state of charge (SOC). Since the fuel cell system efficiency is remarkably lower in the high or low fuel cell output power region, a minimum and a maximum output power level (Pfc_min, Pfc_max) should be determined, in order to operate the fuel cell system efficiently. Meanwhile, the battery SOC should be controlled within a range, such that regenerative braking energy can be effectively absorbed, while ensuring battery life. The flow chart of an optimized load follower control strategy, which is implemented in the Simulink, is illustrated in Fig. 3-5.

A power command, Pcomm, which takes the system loss into account, is produced

from the vehicle pedals, and is connected to the power bus. FC(t) indicates the fuel cell system operation state at each sample time. It is a function of battery SOC and fuel cell's previous state. The fuel cell stack may be turned off, if the battery SOC gets above SOCmax, and the fuel cell stack may be turned on again, if Pcomm is high enough or if the SOC goes below SOCmin. When the fuel cell stack is on, its power output tends to follow the power command, while it may be adjusted by battery SOC, in order to lead the SOC to the centre of its operating range. Furthermore, an SOC-dependent correction factor is defined to let the battery charging or discharging power to be proportional to the difference between the current SOC and the average of SOCmin and SOCmax. For cold start conditions, during the beginning of a drive cycle, the battery needs to be suitably sized, in order to start up the fuel cell. At the same time, the battery must also be capable of maintaining a low speed driving requirement.

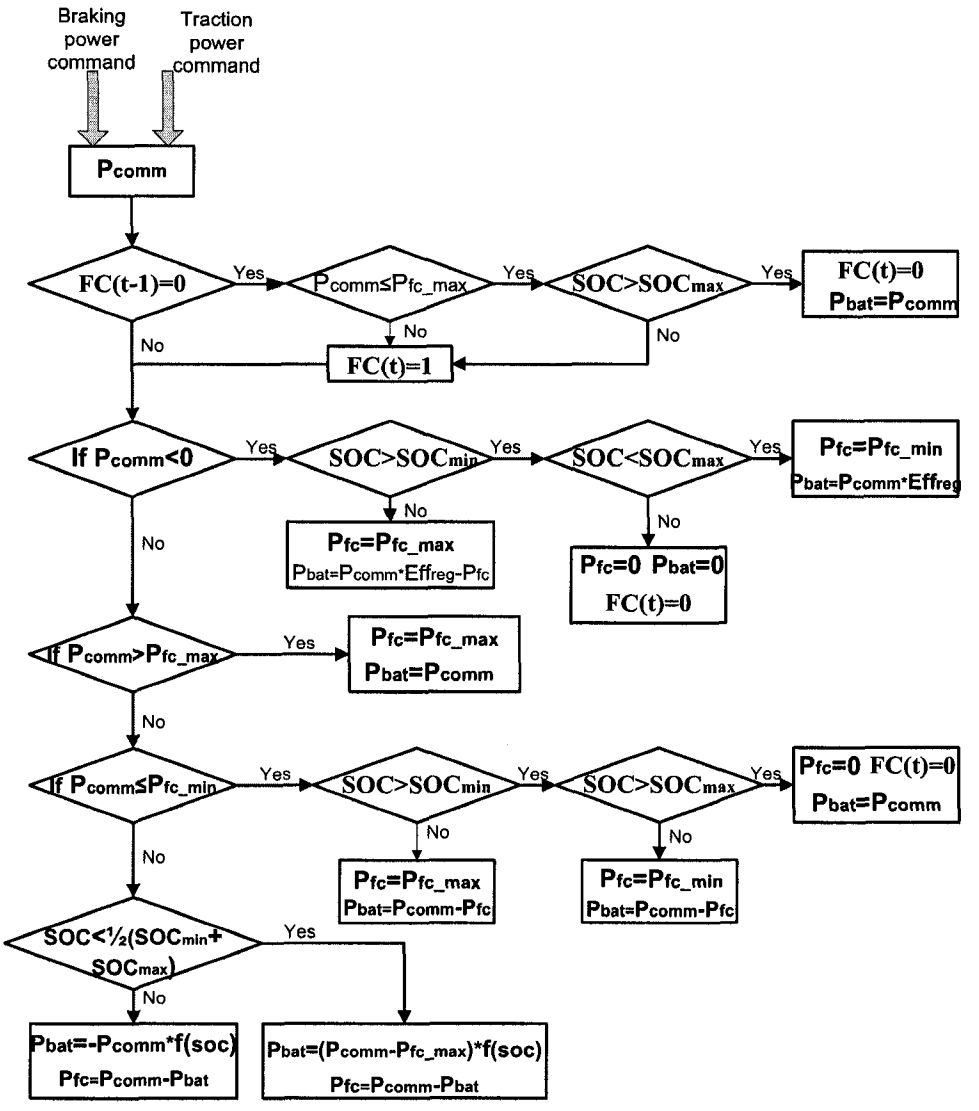

Fig. 3-5 Flow chart of simulated load follower control strategy

Here:

FC (t): State of fuel cell system (0: OFF, 1: ON)

P_{comm}: Vehicle commanded power

P_{fc_max}: Rated power of fuel cell system

P_{fc_min}: Minimum power of fuel cell system

SOC_{min}: The minimum required SOC

SOC_{max}: The maximum required SOC

Effreg: The efficiency of absorbing the regenerative power

f(soc): SOC-dependent correction factor:

$$f(soc) = \frac{0.5(SOC\min + SOC\max) - SOC}{0.5(SOC\max - SOC\min)}$$

3.3.2 Equivalent Consumption Minimization Strategy (ECMS)

The equivalent consumption minimization strategy (ECMS) [19], [20] is a real-time control strategy, developed for parallel HEVs. Under the ECMS, the power distribution between 2 energy sources is determined by minimizing the equivalent fuel consumption at each sample time. It can achieve the overall minimization of fuel consumption by employing a local minimization cost function to minimize equivalent fuel consumption at each instant. This criterion can be expressed as shown in 3-1 [19].

$$\sum \underset{P_{fc(t)}}{Min} \ \dot{m}_{f\_equ(t)} \quad \forall t \tag{3-1}$$

In 3-1, the equivalent fuel flow rate cost function is defined as the sum of the actual fuel consumption rate of the fuel cell (g/s) and the equivalent fuel consumption due to the SOC variation (positive when charging or negative when discharging).

$$\dot{m}_{f\_equ} = \dot{m}_{f\_fc} + f_{soc} \cdot \dot{m}_{f\_bat} \tag{3-2}$$

It should be noted here that this method is based on the charge-sustaining concept, which means that the instantaneous charging or discharging of the ESS will result in future fuel cell output increase or decrease, respectively. Therefore, it associates the power flow through the ESS to an equivalent amount of fuel. This amount of fuel cannot be exactly determined, since it needs prior knowledge of future driving schedule. But an average

factor can be estimated or tuned by accounting for the average efficiency of the energy path. Accordingly the equivalent hydrogen mass flow $\dot{m}_{f\_bat}$ (g/s) is determined as follows [19]:

$$\dot{m}_{f\_bat} = \frac{\overline{SC}_{bat} * P_{bat}}{Eff_{dis\_bat}} \quad \text{(For positive flow: battery discharging)} \qquad (3\text{-}3)$$

$$\dot{m}_{f\_bat} = \overline{SC}_{bat} * Eff_{ch\_bat} * P_{bat} \quad \text{(For negative flow: battery charging)} \qquad (3\text{-}4)$$

Here, P_{bat} is the instantaneous battery output power, $\overline{SC}_{bat}$ (g/kWs) represents the average amount of hydrogen needed to store 1 kWs of electrochemical energy in the battery, using the fuel cell as a charger. This can be obtained from the simulation data from the vehicle model. An SOC weighting factor, f (soc), as shown in 3-2, is added, to further regulate the power split, according to the deviation between the actual and target SOCs. A penalty function can be designed to embody the desired characteristics of ESS, as shown in Fig. 3-6.

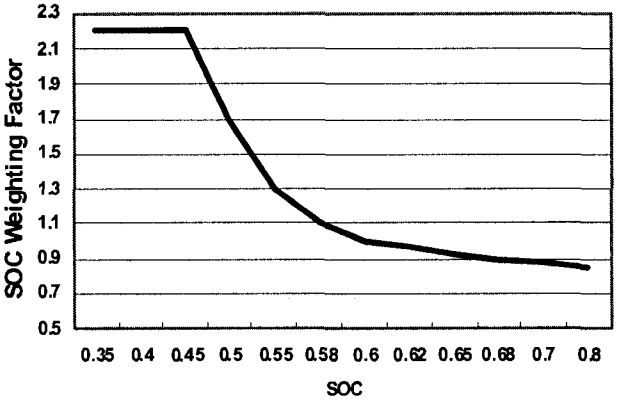

Fig. 3-6 SOC weighting factor f(soc) for ECMS

As is clear, the SOC weighting factor will be close to 1 and tend to be flat when the SOC is close to the target value (0.6, in this case), in order to maintain the optimal

maintain the optimal power split. The flow chart, shown in Fig. 3-7, illustrates the principle of the ECMS algorithm.

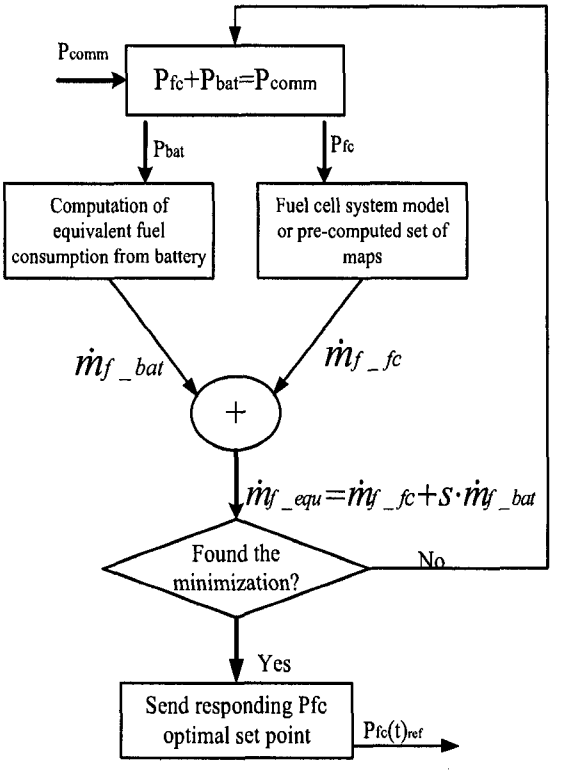

Fig. 3-7 Principle of the applied ECMS algorithm

First, according to the power demand and component limits, the valid range for the combination of fuel cell power output and battery output is monitored. Next, the fuel consumption rate from the fuel cell, $\dot{m}_{f\_fc} = f(P_{fc})$, can be obtained, by a pre-computed set of maps from the fuel cell system model. It is worth noting here that temperature is also an important factor to be related to this function. Meanwhile, the equivalent fuel consumption rate of the battery can also be calculated from 3-3 and 3-4. The total fuel consumption cost function, $\dot{m}_{f\_equ}$, is then computed from 3-2. Thereafter, the corresponding net fuel cell output power is chosen at each sample time, which yields the minimum value of $\dot{m}_{f\_equ}$.

3.3.3 SIMULATION RESULTS AND ANALYSIS

The overall FC-HEV simulation is implemented by connecting each of the modeled subsystems. The power sharing control algorithm is implemented in Simulink, and is included in the model, to provide power management. The power components are sized for power requirements of a mid-size sedan as summarized in Table 3-1. A total of 3 driving patterns are chosen, to test the control strategy performance. They are the Urban Dynamometer Driving Schedule (UDDS), Highway Fuel Economy Test (HWFET) cycle, and the high speed and high acceleration US06 highway cycle.

Table 3-1 Power component parameters

Component	Description
Fuel Converter	50kW net hydrogen fueled fuel cell stack.
Motor/ Controller	75kW AC Induction motor
Energy Storage System	Ovonic45Ah NiMH battery (25 modules)

The results of instantaneous power split between the fuel cell and the battery, as well as the battery SOC for both control strategies, are shown in Fig. 3-8. The increasing and decreasing rates of power are limited at 2kW/s and -3kW/s, respectively, for both strategies. It can be clearly noted that ECMS presents much better performance in charge sustaining mode, where the battery SOC can globally maintain close to the target SOC (0.6 in this case). This characteristic is insensitive to the driving cycle, and can be flexibly adjusted through the SOC weight factor. For the load follower scheme, the fluctuation of the SOC is more obvious, although it can be controlled to be between the minimum and maximum SOC level. For example, in the UDDS cycle, frequent braking

modes lead to the increase in battery SOC, and will continue to increase in the ensuing cycles, until it reaches its maximum level, while in the US06 cycle, the SOC tends to decrease in the ensuing cycles, until it reaches its minimum level.

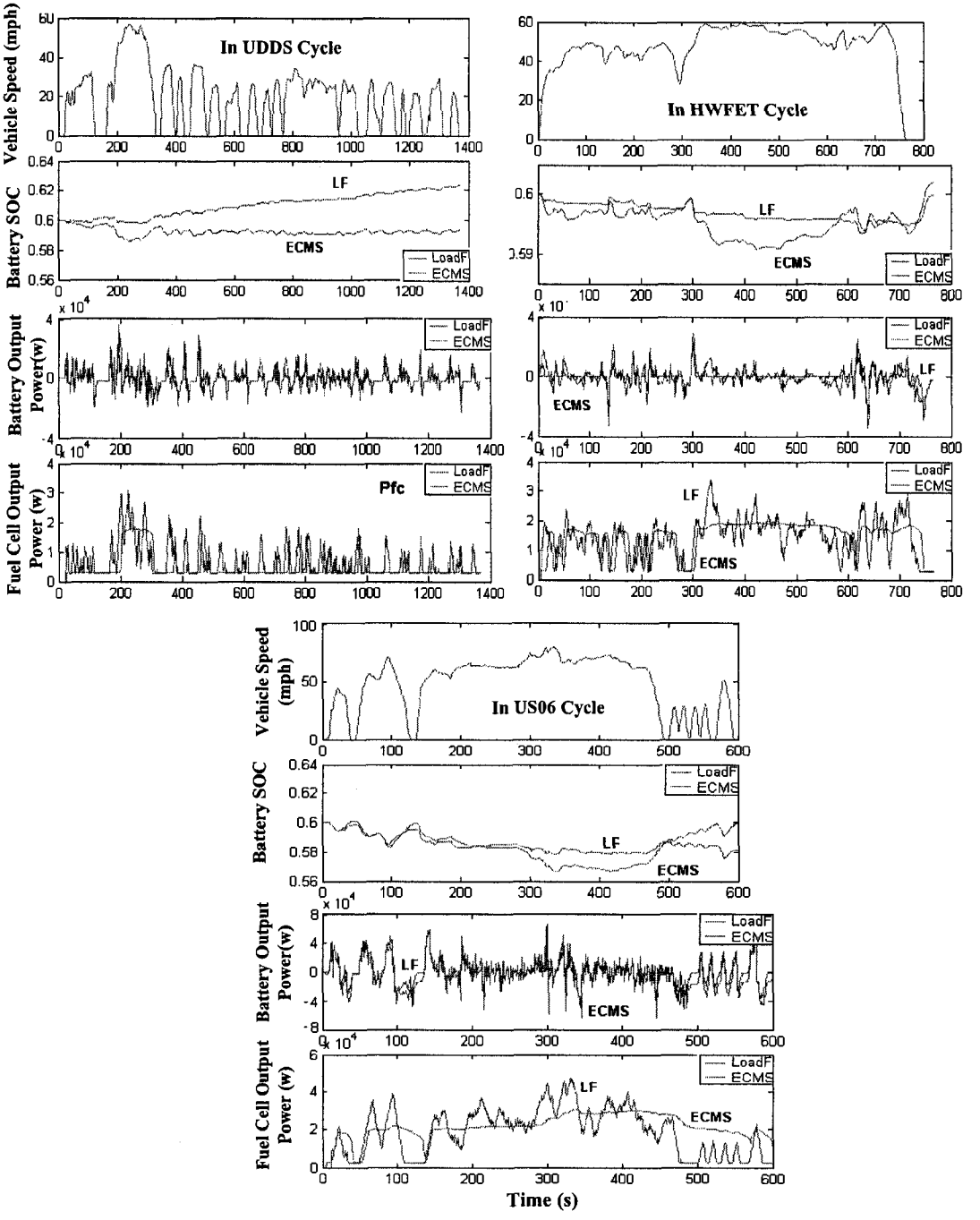

Fig. 3-8 SOC and power flows in UDDS, HWFET, and US06 driving cycles

Fig. 3-9 further illustrates the battery SOC performance in 6 continuous UDDS and US06 driving cycles, for both control strategies. With ECMS, under both UDDS and US06 driving conditions, the battery SOC can be globally maintained close to the target level. While for Load Follower, the battery power tends to fluctuate between the maximum and minimum SOC limits. Hence, there is a risk of battery over-charging or over-discharging.

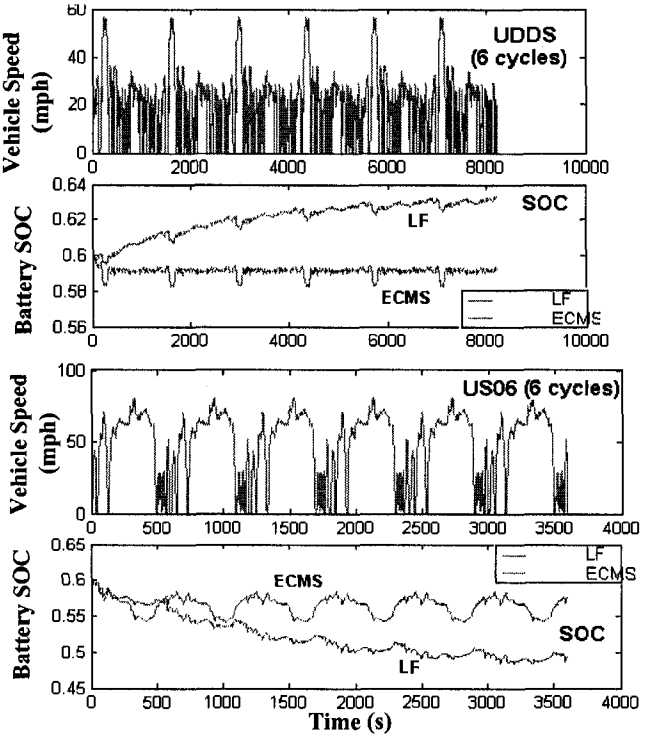

Fig. 3-9 Battery SOC in 6 continuous UDDS and US06 driving cycle

In terms of system power flow, it can be observed that during the UDDS drive cycle, ECMS allows the battery to utilize most of its energy, irrespective of whether it is charging from regenerative braking power or discharging. As for fuel cell power output, with ECMS, the fuel cell system is often operated at a low, constant power level, where the efficiency is high. In contrast, in case of the load follower scheme, the output power

follows the load from the drive cycle more frequently, and thereby, the peak power demand is much higher than that with ECMS. In the case of cold start, the load follower scheme will solely let the battery provide power, due to the low efficiency of the fuel cell at low temperatures. Similarly, the ECMS will automatically limit the fuel cell output to a very low or off level, because steeper fuel consumption in low temperatures will narrow the valid power range of the fuel cell, according to the algorithm. Fig. 3-10 and Fig. 3-11 display the fuel cell system operating points for the UDDS and US06 drive cycles, operating under the load follower scheme and ECMS, respectively. As mentioned earlier, it is found that the ECMS strategy shifts the majority of operating points towards higher efficiency, and the peak power command significantly reduces, compared to load follower.

In terms of the battery efficiency, from the simulation results of Fig. 3-12, it can be found that the battery efficiency with Load Follower is higher than that with the ECMS. This is because the charging and discharging frequency under ECMS operation is higher than that with the load follower, which creates higher losses. Therefore, to some extent, the ECMS sacrifices some battery efficiency to achieve higher fuel cell efficiency.

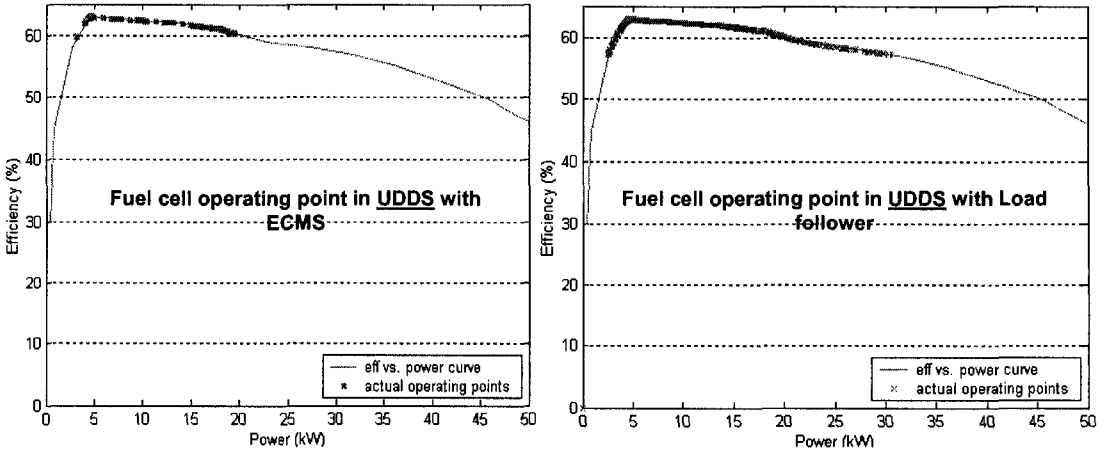

Fig. 3-10 Fuel cell system operating points in UDDS with two control strategies

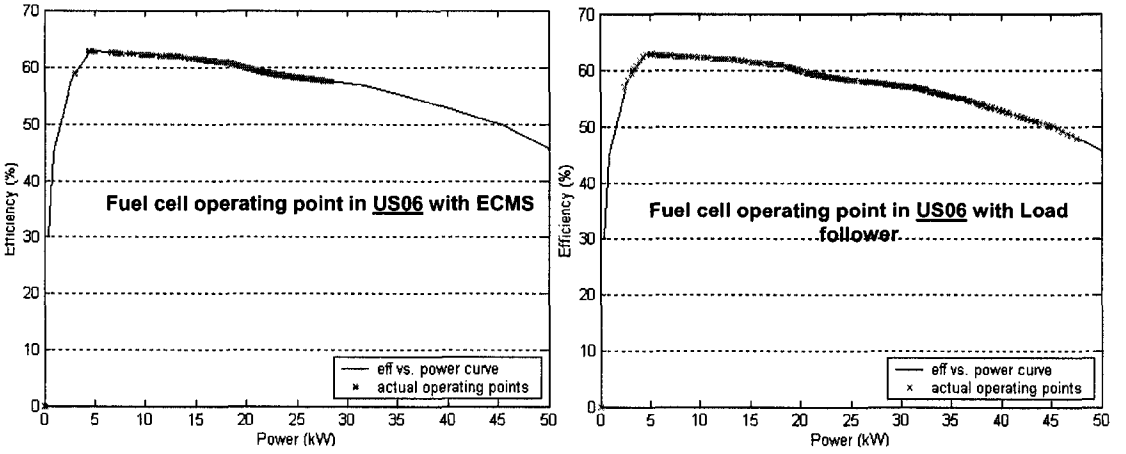

Fig. 3-11 Fuel cell system operating points inUS06 with two control strategies

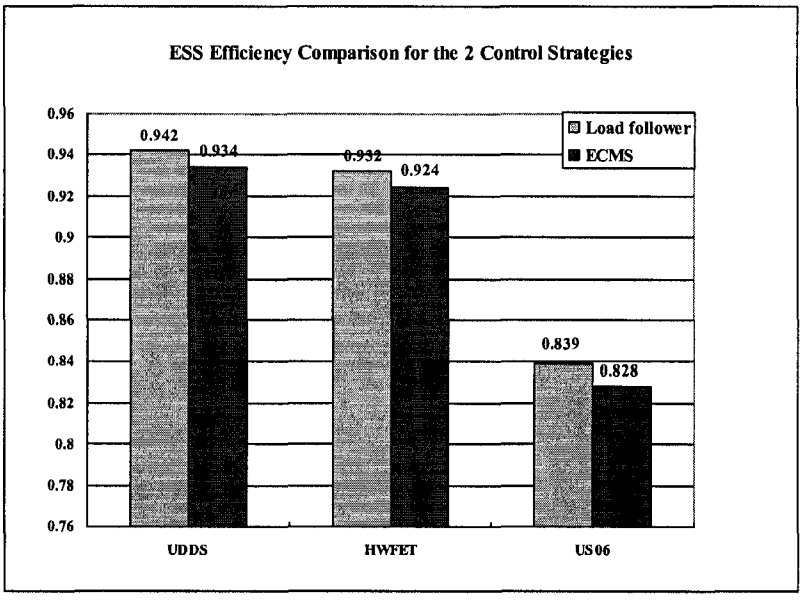

Fig. 3-12 Battery efficiency comparison with two control strategies

Fig. 3-13 compares the fuel economy results between the ECMS and the load follower scheme, for the 3 types of drive cycles under test. The fuel economy is evaluated in miles per gallon equivalent (MPGe). Furthermore, the simulation times are selected to be 5 continuous driving cycles, and the tests are conduct with SOC correction to achieve

a fair comparison. As can be seen, the fuel economy with ECMS is better than that with load follower, for city (UDDS) and aggressive (US06) drive cycles. At the same time, in the HWFET cycle, the advantage or disadvantage is not obvious. This signifies a modest difference between the 2 strategies with regards to fuel economy, especially for nearly constant speed conditions.

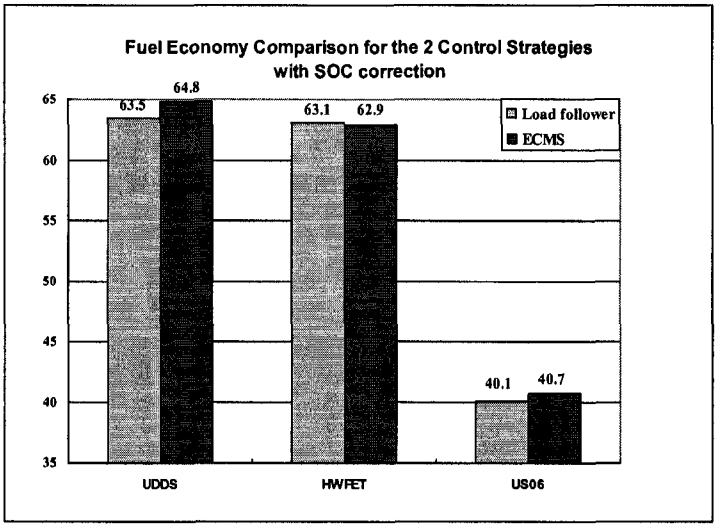

Fig. 3-13 Fuel economy comparison for the 2 control strategies

To test the vehicle dynamic performance, specific acceleration tests and gradeability tests were conducted for both the control strategies. The gradeability performance tests results are summarized in Table 3-2.

Table 3-2 Gradeability performance comparison

Control Strategy	Gradeability Test (55mph for 10s, 1350 kg)
Load Follower	27.7%
ECMS	24.5%

It is found that the load follower scheme performs better in the gradeability test than ECMS. This means that during high power requirements, or for more aggressive driving conditions, the load follower splits the power more flexibly, in order to follow the power demand. The acceleration test results for both the strategies were found to be almost similar (7.6s for 0-60 mph, 3.7s for 40-60 mph, and 15.5s for 0-85 mph).

3.4 SUMMARY

This chapter compared and analyzed the control performances of 2 optimally designed power control strategies for FC-HEVs. Both strategies are implemented in Simulink and analyzed in ADVISOR. Both the strategies investigated are real-time control strategies, which can be implemented practically. The load follower scheme determines the instantaneous power split between the fuel cell and the battery according to a set of rules, considering the power requirement from the power bus and the operation state of the battery and fuel cell. The ECMS scheme is based on a static optimization method that utilizes an analytical formulation, to find the best power split, in order to minimize the hydrogen consumption at any sample time.

The simulation results indicate that the ECMS presents a better fuel economy than the load follower scheme in most driving conditions, especially in the urban driving cycle. But the advantages of the ECMS become smaller during constant high speed driving conditions. The battery efficiency with ECMS seems to be lower than that with load follower, due to frequent charging and discharging, although ECMS shows its robustness in maintaining the SOC level under different driving conditions. In addition, it is found that usage of the ECMS strategy can lead to the shifting of fuel cell operating points to high efficiency regions, and reduces its peak power demands. However, the vehicle

dynamic performance seems better with the load follower scheme, since it can follow the load change more flexibly. Therefore, it can be concluded that the ECMS strategy sacrifices the vehicle performance to some extent, in order to achieve better fuel economies.

It should also be noted that the load follower scheme is less dependent on the component parameters. Therefore, the optimization can be performed by simply making the rules more reasonable and suitable to the vehicle configuration and driving conditions, or by taking more operating modes into consideration, such as cold start and battery over-discharging protection, although it will increase the complexity of implementation. In comparison, the ECMS strategy is found to be self-adaptive to power train component characteristics and efficiency factors. The tunable SOC weighting factor also provides vehicle flexibility to adjust the strategy according to driving conditions and control limits. These factors also make the ECMS easier to be applied to other hybrid configurations, such as fuel cell/ultra-capacitor powered hybrid vehicles. At the same time, the ECMS is very sensitive to model parameters, such as SOC weighting factor and estimation of average specific fuel consumption. Thus, the accuracy of the model formulation is crucial to the overall control performance of ECMS. Hence, the ECMS scheme can be further improved by optimizing the above-mentioned parameters and taking into account additional vehicle performance factors, especially in the case of high power demands.

CHAPTER 4

LOW-LEVEL POWER ELECTRONICS AND CONTROL CIRCUIT DESIGN

4.1 INTRODUCTION

This chapter will present the low level power circuit design and control of the power train system for a FC-HEV. As illustrated in Fig.1-9 of the proposed power train system configuration, the power conditioner between the fuel cell and the battery system plays a crucial role, in order to provide protection of power components and matching the voltage levels of different power sources to the main DC bus. Meanwhile, it will also provides control of the demanded power according to the reference power value (usually transfer to reference current) from the system supervisory controller, as discussed in last chapter.

In the ensuing sections, the power train topology selection based on the component characteristics and power requirements will be discussed. Two popular topologies are considered based on 2 options of hybridization degree selection. Thereafter, the circuit modeling of power components in PSIM software as well as the power converter design will be introduced. Finally, the control scheme design and simulation-based analysis will be presented.

4.2 POWER TRAIN CONFIGURATION

An ideal topology for FC-HEV is that both the fuel cell system and the ESS are

directly connected to the propulsion motor. This seems to be most efficient and economical configuration. However, this configuration is applicable only if both the fuel cell and ESS output voltages match the voltage level of the DC bus, which in turn, needs be set to a level suitable for usage with the motor system. The fact is that fuel cell output is usually lower than the DC bus requirement, and tends to depict a wide variation during operation, or the voltage between the fuel cell and battery does not match [23]. This leads to low efficiency and reliability, and proves to be extremely complicated when providing power distribution control in a hybrid configuration.

Therefore, a DC/DC converter is necessary for power conditioning between the 2 power sources and the DC voltage bus, which is in turn connected to the propulsion system. In general, there are 2 options of power train structures, based on the position of the DC/DC converter, as shown in Fig. 4-1. In topology-A, the fuel cell is connected to the high voltage DC bus through a unidirectional DC/DC converter, while the battery is directly connected to the DC bus. In this condition, the fuel cell output can be directly controlled, while the battery output voltage needs to match the DC bus voltage level. In topology-B, the fuel cell is directly connected to the DC bus, while the battery is connected to the DC bus through a bi-directional DC/DC converter.

The utilization of a bi-directional converter between the battery and DC bus allows more flexibility to the battery, because such an arrangement not only reduces the voltage requirement of the battery, but also provides the freedom to control its state of charge (SOC). Since the fuel cell is directly connect to the high voltage DC bus, a large sized stack or voltage level is required, and the control of fuel cell power can only be achieved indirectly, by controlling the battery output, or through internal fuel control. The use of 2

high power converters for both battery and fuel cell generally is not economical from the point of view of cost and size consideration.

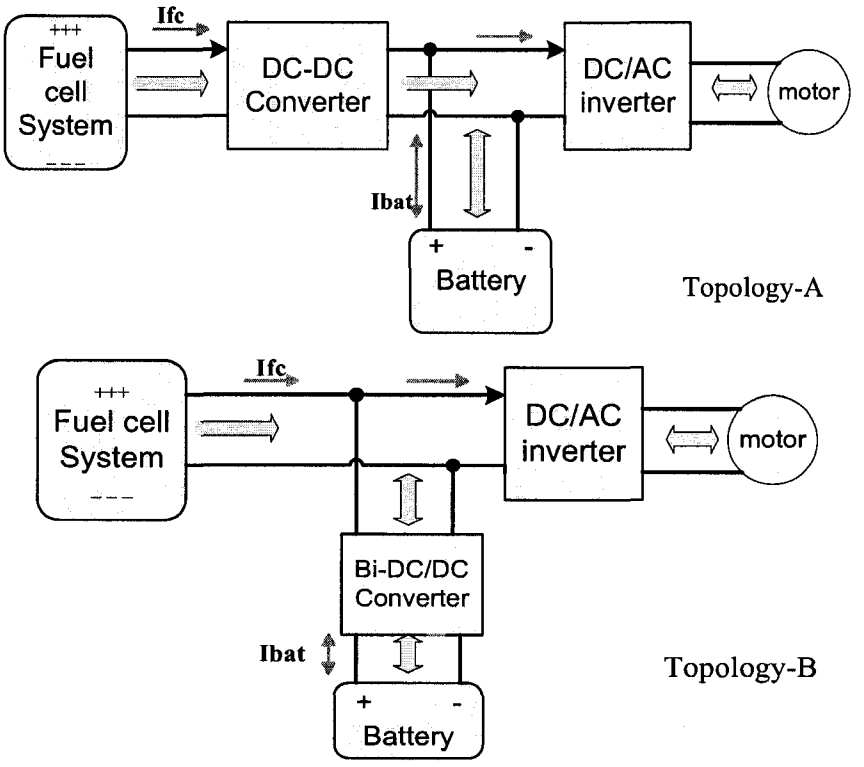

Fig. 4-1 Power train topological options for FC-HEVs

In this thesis, the topology selection is considered according to the hybridization degree. The hybridization degree here is defined as the ratio between the fuel cell rated power and the peak power of the traction motor. A higher hybridization degrees leads to better fuel economy, but requires a large sized fuel cell, which in turn leads to high cost. Here, the sizing of a mid-size SUV type vehicle is considered for study, since SUVs are one of the most popular and fuel inefficient vehicle type. Moreover, SUVs provide more potential to arrange the power component size, since they have large space. Two specific cases of hybridization degrees are selected based on the peak/average power requirement of a mid-size SUV (140kW/50kW, in this case), as described in Table 4-1.

Table 4-1 Two cases of hybridization for a mid-size SUV

	Fuel Cell Size (PEM)	Battery Size (Ni-MH)	Power train type
Case-1	60kW	25 modules	Topology-A
Case-2	80kW	20 modules	Topology-B

For case-1, power train topology-A is chosen, because the fuel cell size is relatively small and the voltage level for a 60kW PEM fuel cell (200-300V) does not match the DC bus voltage (300-450V). Therefore, the DC/DC converter allows a downsized fuel cell and can allow complete control. At the same time the rated voltage of the 25 battery pack cells can be set to be around 400V, which represents the DC bus voltage level. For case-2, which has a larger fuel cell and smaller battery pack, the 80kW fuel cell (300-400V) can be directly connected to the DC bus, while a bi-directional DC/DC converter is needed for the battery, to match the voltage level as well as to control the battery charging and discharging performance.

4.3 POWER COMPONENT MODELING

4.3.1 FUEL CELL SYSTEM

To obtain the electrical characteristics of the fuel cell, its circuit model is represented by a look-up table and controlled voltage source, which provides the fuel cell voltage corresponding to the current drawn from the fuel cell, as shown in Fig. 4-2. The diode at the fuel cell output is to prevent the negative current going back into the stack, and an on-off controller is added, to ensure that the fuel cell operates in an acceptable area.

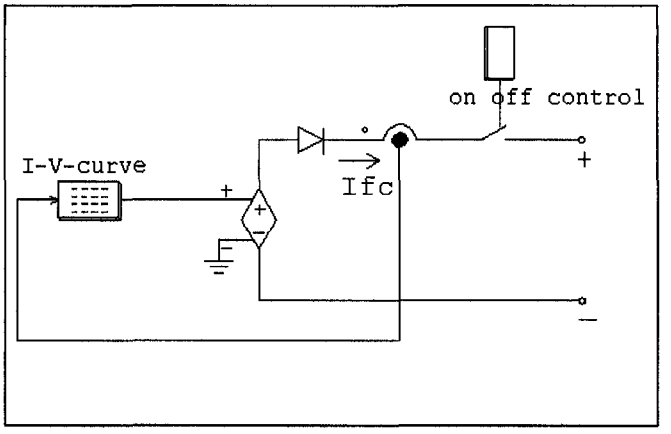

Fig. 4-2 Fuel cell model

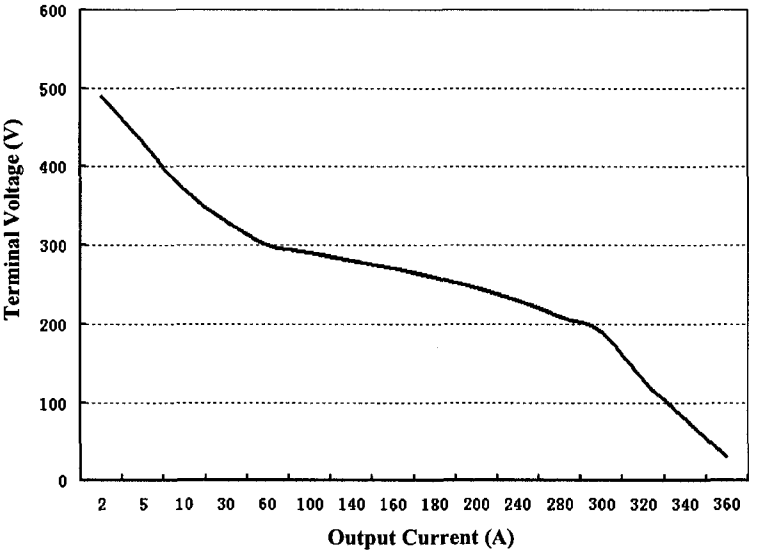

Fig. 4-3 V-I polarization curve of a 60kW PEM fuel cell stack

The fuel cell V-I characteristic is normally portrayed in the form of a polarization curve, which is determined by the relation between cell voltage and current density, as described in chapter 1. Fig. 4-3 illustrates the V-I curve of a 60kW fuel cell. The stack temperature and membrane water content affect the fuel cell voltage. The voltage decreases as higher current is drawn from the fuel cell, due to the fuel cell electrical resistance, inefficient reactant gas transport, and low reaction rate [5]. Lower voltage

indicates lower efficiency of the fuel cell, and the maximum current drawn from the fuel cell is defined as the current at which the maximum output power is achieved. Many cells are typically combined in a stack, to satisfy the power requirement of the target application.

4.3.2 BATTERY SYSTEM

The battery system is modeled based on a typical RC model, as described in chapter 2. This model consists of a voltage controlled voltage source in series with an internal resistor, as shown in Fig. 4-4. The battery output voltage is determined by the battery SOC, through a look-up table. The relation between battery cell-voltage and SOC is obtained from validated experimental data, as shown in Fig. 4-5. The battery SOC is calculated as the energy present in the battery divided by the maximum energy capacity (Ah) of the battery pack, as given in 4-1.

$$SOC = \frac{Capacity_{max}(Ah) - Ah\_used}{Capacity_{max}(Ah)} \tag{4-1}$$

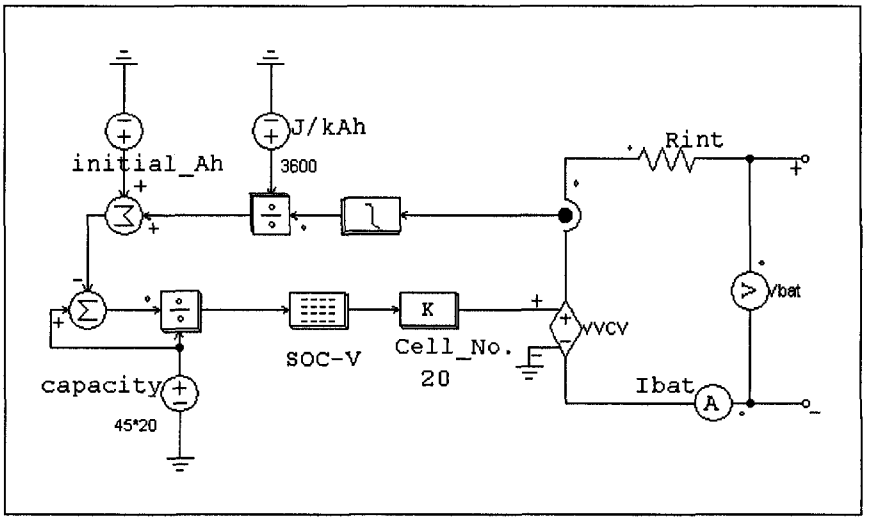

Fig. 4-4 Battery model

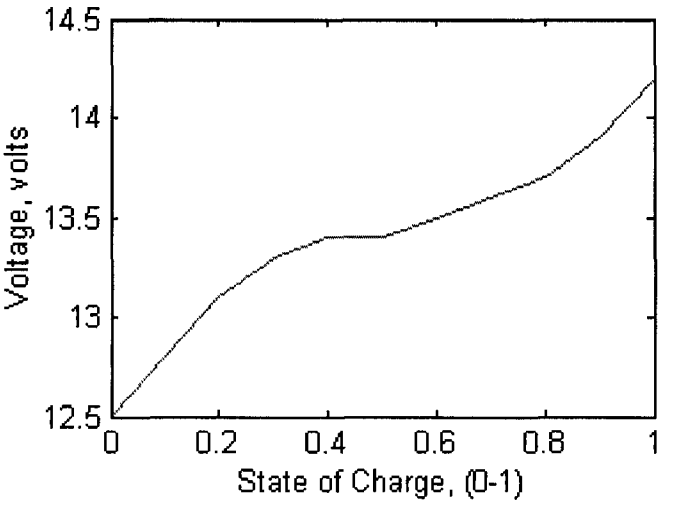

Fig. 4-5 SOC versus terminal voltage curve for Ni-MH battery cell

4.3.3 PROPULSION SYSTEM

An active load is used to model the demanded power from the propulsion system, which avoids the complicated modeling of motor and motor controller. The propulsion system is modeled as a controlled current source, drawing current from the system, as shown in Fig. 4-6. Various driving scenarios are translated to corresponding power requirements through a look-up table with respect to time. This relation data can be obtained from the vehicle system level simulations. The motor required current can thereby be obtained after divided by the DC bus voltage.

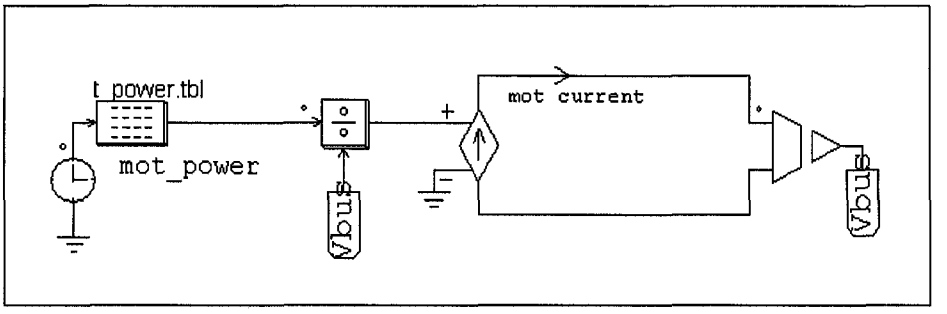

Fig. 4-6 Propulsion system model

4.4 POWER CONVERTER SELECTION

4.4.1 POWER CONVERTER SELECTION FOR TOPOLOGY-A

A high-power unidirectional DC/DC converter is needed to interface the fuel cell to the propulsion system, in topology-A. The main role of this converter is to boost the fuel cell voltage to be within the operating range of that of the DC bus, and to regulate the fuel cell output power according to the high-level control strategy. Another significant goal is to achieve lower fuel cell output current ripple at high frequencies. This is of immense significance, because fuel cell systems prefer lower levels of current ripple, which ultimately results in prolonged life time of the system.

For converter design or selection, compromises should be made in considering size, cost, efficiency, input voltage range, and other parameters. Possible choices mainly include typical boost converter, which uses least number of switch components, depicts high reliability, and continuous input current. At the same time, the disadvantage is obvious, due to the large size of passive components. In addition, the current ripple is high and the power loss limits the overall efficiency. There also exist a series of high power converters with isolated topologies, such as the forward converter with step-up transformer. These converters usually contain transformers and more than 2 semiconductor devices, which lead to inadequate reliability and high cost. Besides, the output/input ratio in this application is smaller than 2 and electrical isolation is not very necessary in such a high-voltage system. Furthermore, when considering the *Cuk* converter, it requires much more passive elements, which is not very attractive.

Based on above overview, a high-power interleaved boost converter, as shown in

Fig. 4-8 [24] [25], is selected for this application, which helps reduce the volume and weight of the inductor and greatly improves the current ripple and reliability. As can be seen, this converter is modified form of the typical boost converter with dual phases. The 2 power switches (IGBT) S1 and S2 have 180° phase difference in a cycle, whereby the fluctuation of the input current can be greatly reduced. This is because the 180° phase difference between the 2 inductor currents minimizes the overall ripple. In this way, the 2 inductors can be designed to adopt much less inductance value as well as half the current rating, correspondingly. Table 4-2 provides a simulation-based comparison of a 60kW DC/DC converter, using the interleaved converter topology.

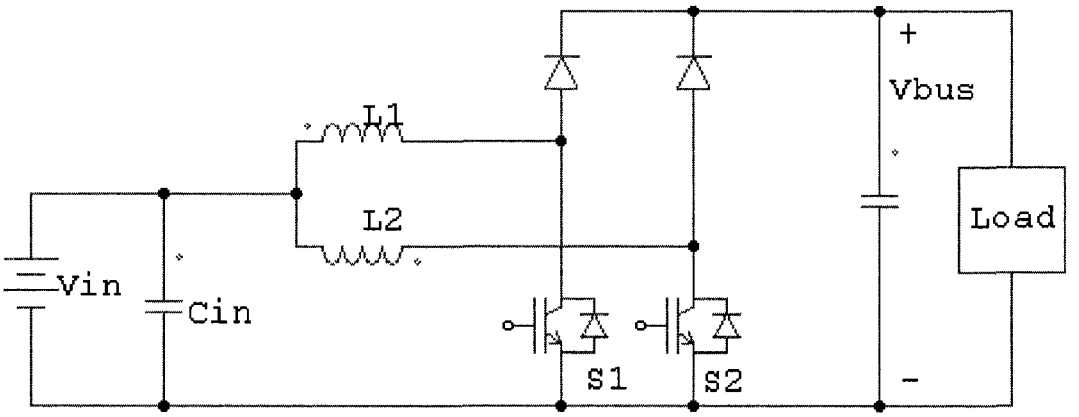

Fig. 4-8 Topology of the interleaved boost converter

Table 4-2 Comparison of 2 types of boost converters

	Inductor size	Input Capacitor size	Input current ripple	Average efficiency
Typical Boost	120uH	220uF	6%	92%
Interleaved Boost	60uH	120uF	3%	96%

4.4.2 POWER CONVERTER SELECTION FOR TOPOLOGY-B

In case of topology-B, a bi-directional DC/DC converter is needed to interface a smaller size battery pack to the high voltage DC bus, and to regulate the output power from the battery or the fuel cell. Ref. [18] reviews the candidates for the bi-directional converter, from which a boost type half bridge DC/DC converter is selected, as shown in Fig. 4-9. When the battery operates in the charging mode, S1 switch and S2 diode work as a buck converter, to charge the low-voltage battery. When the battery operates in the discharging mode, S2 switch and S1 diode work as a boost converter, which delivers the battery power to the high-voltage DC bus.

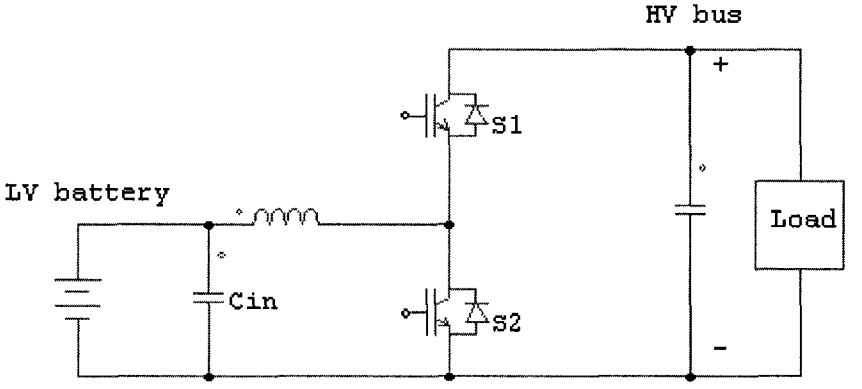

Fig. 4-9 Half bridge bi-directional converter topology

In contrast to a buck-boost type converter, described in [18], the half bridge topology only needs half the number of active components to achieve the same performance, which leads to higher efficiency. The average efficiency for 60kW level is found to be 94%. Also, compared to the *Cuk* converter, the inductor value of the half bridge converter is only 50%, and the current-rating of the active components is much lower. The isolated type of topology is not used due to additional cost and losses of the transformer. Moreover, the isolation is not necessary in this application.

4.5 CONTROLLER DESIGN AND SIMULATION

4.5.1 CONTROL AND SIMULATION FOR TOPOLOGY-A

For topology-A, the power drawn from the fuel cell is controlled by controlling the fuel cell output current. The power demand from the supervisory controller is referred to the P-I curve, to derive the fuel cell reference current. Since the motor power is controlled by the motor-controller, the battery power can be indirectly controlled by the difference between the fuel cell power requirement and the motor power demand. Since the size of the battery is big enough to provide around 380V terminal voltage (25 Ni-MH cells, with 13.6V/cell rated voltage), neither the converter output voltage nor the DC bus voltage needs to be controlled. This simplifies the control requirements, which increases the reliability. The circuit control scheme is illustrated in Fig. 4-10, and the overall circuit diagram is illustrated in Fig. 4-11.

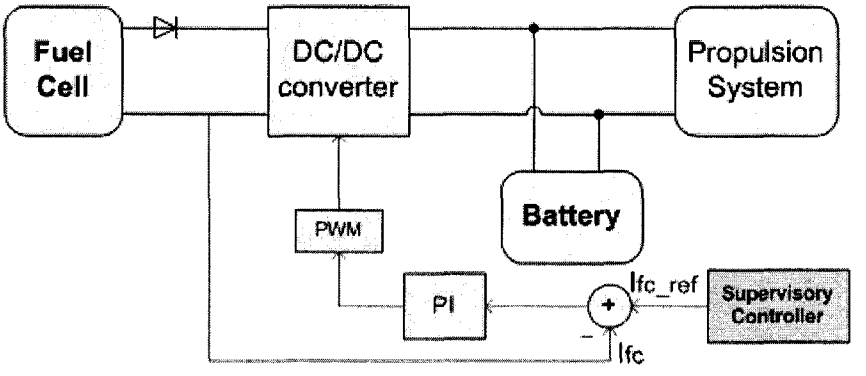

Fig. 4-10 Circuit control scheme diagram for topology-A

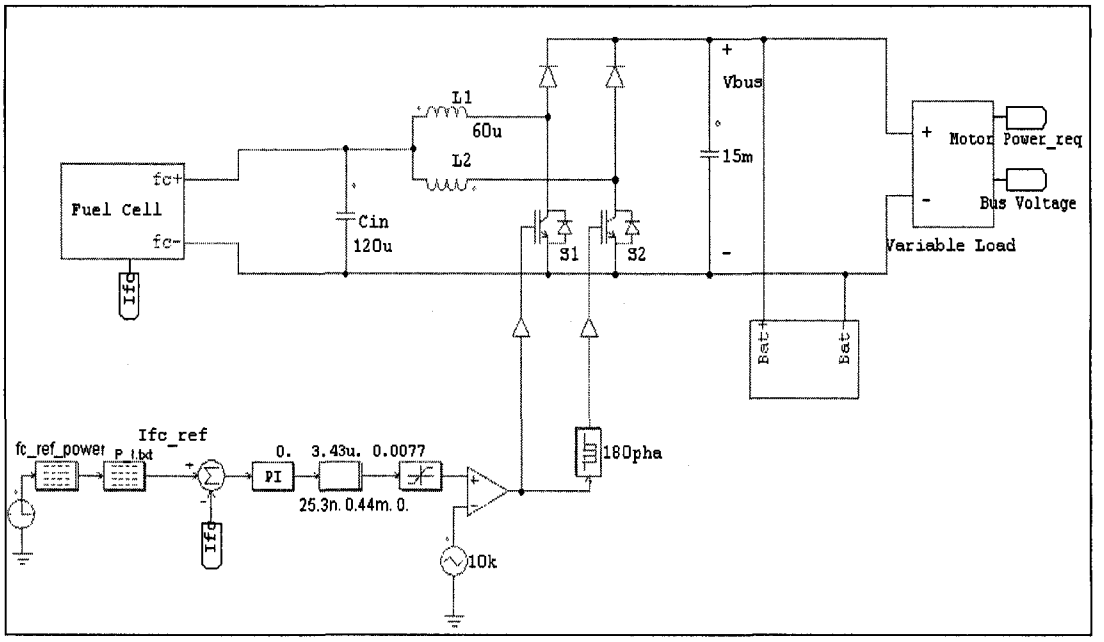

Fig. 4-11 Circuit diagram for topology-A

In the 60kW interleaved boost converter, the inductor is designed to be 60uH. A 120uF input capacitor is used to further reduce the current ripple. The switching frequency is set to be 10 kHz. According to the open loop transfer function, shown in (4-2), a PI type-2 controller is designed, to regulate the current loop as given in 4-3. The closed loop bode plot is shown in Fig. 4-12, in which the current loop crossover frequency is set to be 1 kHz with a 50° phase margin.

$$G_{id}(s) = \frac{RCV_0 * s + 2V_0}{RLC_m * s^2 + L * s + RD_f^2} \tag{4-2}$$

$$Gctr = \frac{0.12m + 1.6}{2.5us^2 + 0.8ms} \tag{4-3}$$

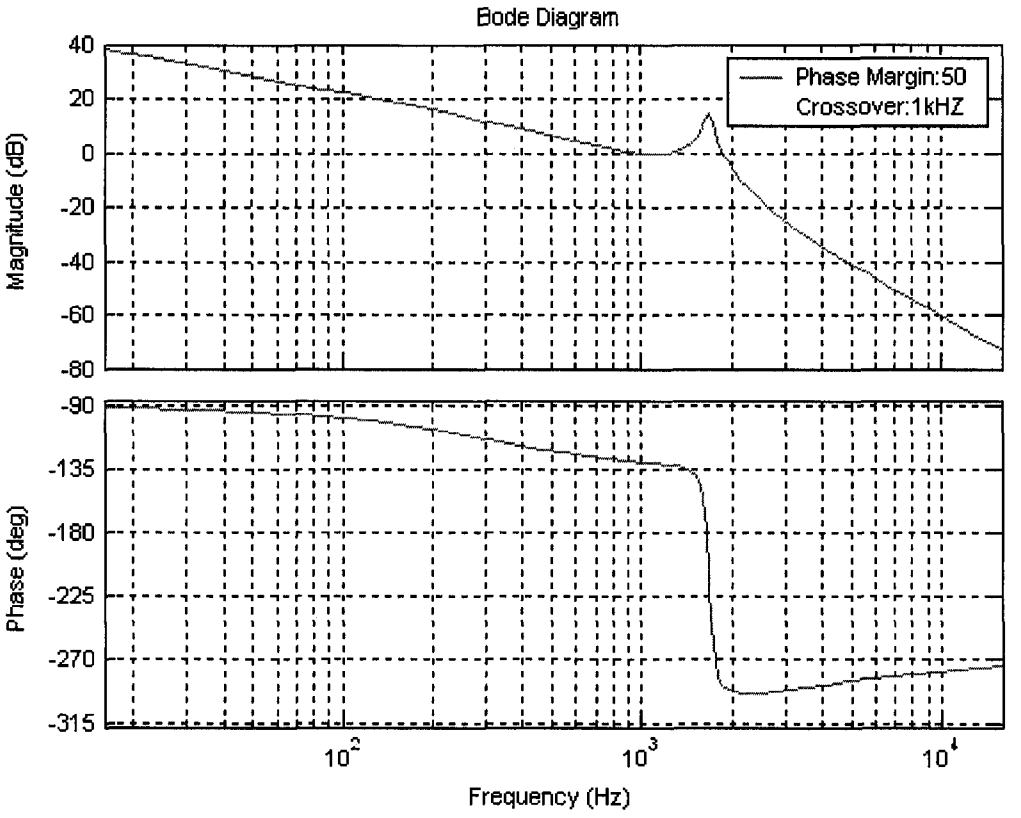

Fig. 4-12 Plot for the boost converter current loop

The fuel cell response to a 50kW power requirement is shown in Fig. 4-13, and the 2 inductor transient currents are shown in Fig. 4-14. The two 180° phase difference inductor currents reduce the overall ripple, as discussed earlier. Fig. 4-15 illustrates the system transient performance of current and power distributions during an acceleration and deceleration period, during a section of the UDDS drive cycle. The power distribution command is provided by the supervisory controller, which uses the load follower control strategy, as designed in chapter 3. It indicates that, with a converter directly regulating the fuel cell power, the reference signal from the load follower control strategy can be easily implemented by low-level control. It is found that the fuel cell current can follow the current request very closely, with negligible overshoot or error.

Thereby, the battery output current can be indirectly regulated, while the DC bus voltage is stabilized by the battery pack.

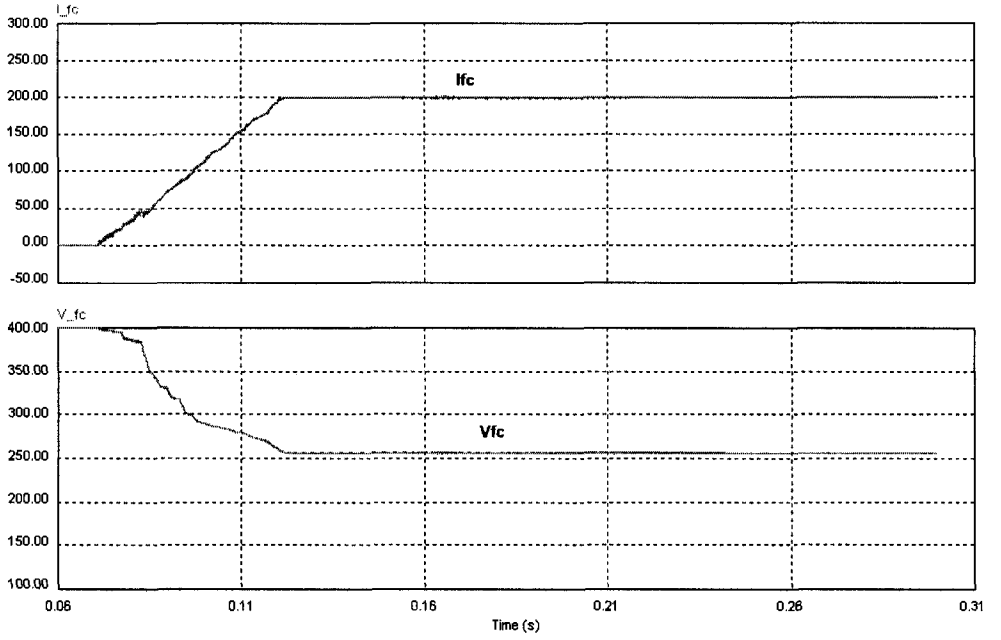

Fig. 4-13 Fuel cell output response to a 50kW power command

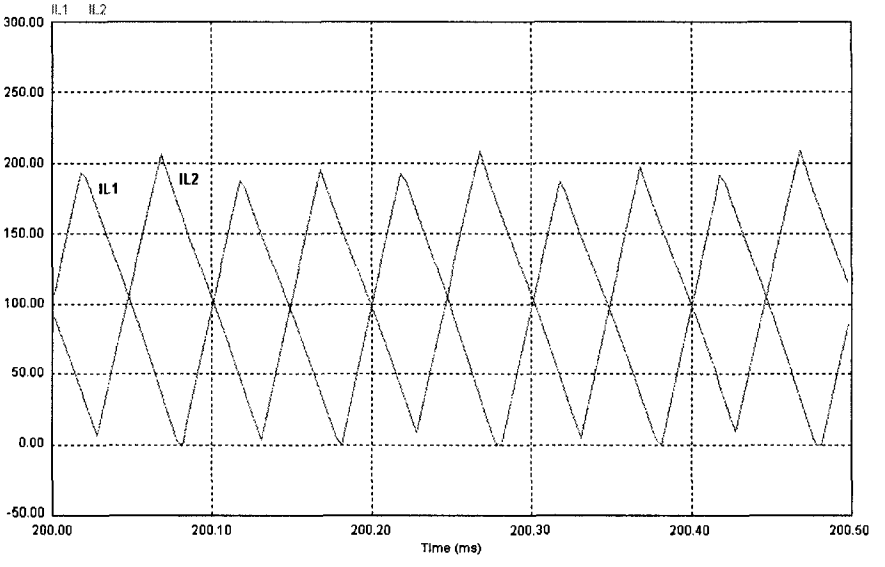

Fig. 4-14 Inductor current of the interleaved boost converter

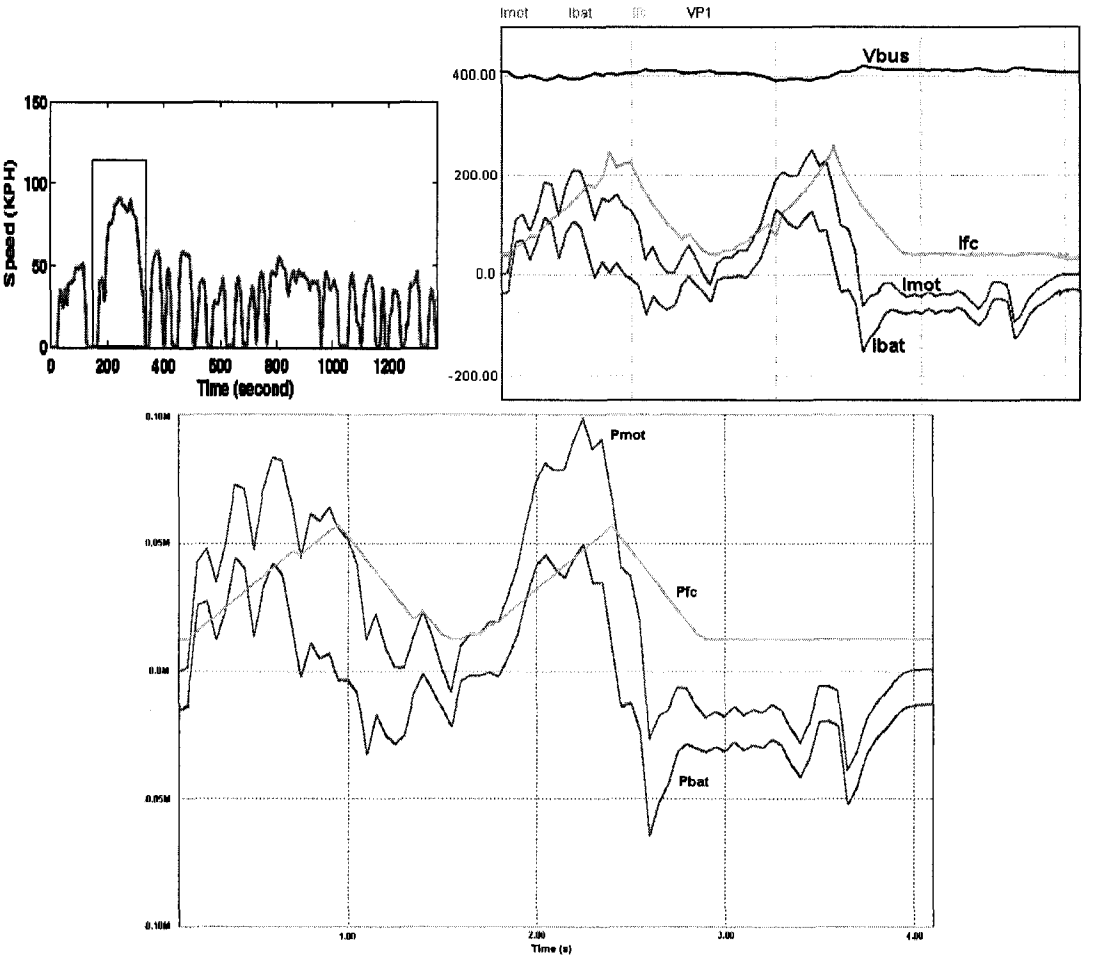

Fig. 4-15 Topology-A transient performance over a portion of the UDDS drive cycle

4.5.2 CONTROL AND SIMULATION FOR TOPOLOGY-B

As aforementioned, in topology-B, a half-bridge bi-directional DC/DC converter is connected between the battery and the traction motor, and a large sized fuel cell is directly connected to the DC bus. The power circuit control scheme is illustrated in Fig. 4-16, and the system circuit schematic is shown in Fig. 4-17. When the battery discharges, the power switch S1 operates, to boost the battery voltage; when battery needs to be charged, the converter operates as typical buck converter mode, wherein S2 operates. The power flow direction through the converter is changed by switching the operating modes,

which is determined by the difference of the load/battery currents and the reference battery output power. Two PI controllers are designed for boost and buck converter modes. In the boost mode, the DC bus voltage is controlled to manage the fuel cell output power, and in the buck mode, the battery output voltage is controlled to regulate the battery output power.

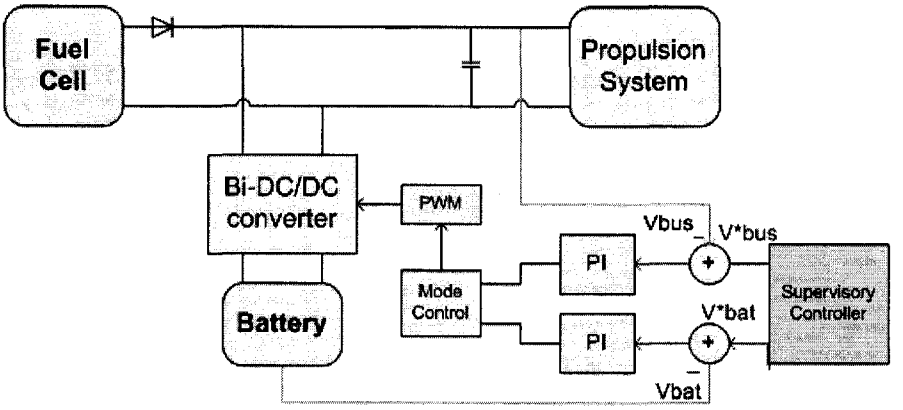

Fig. 4-16 Circuit control scheme for topology-B

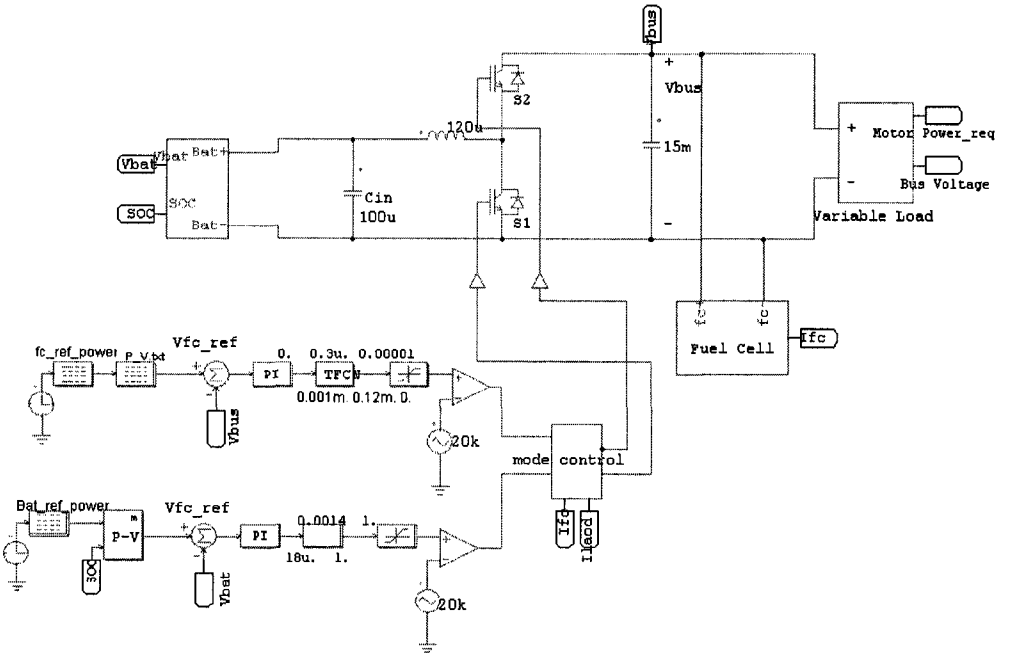

Fig. 4-17 Circuit diagram for topology-B

The switching frequency is set to be 20 kHz, to satisfy the fast response of the battery, compared to the fuel cell, and the bandwidth of the voltage loop is selected to be 2 kHz. Fig. 4-18 and Fig. 4-19 show the battery output response to a 26kW discharging power demand and a 40kW charging demand, respectively, from which the battery power can be regulated with acceptable overshoot and ripple.

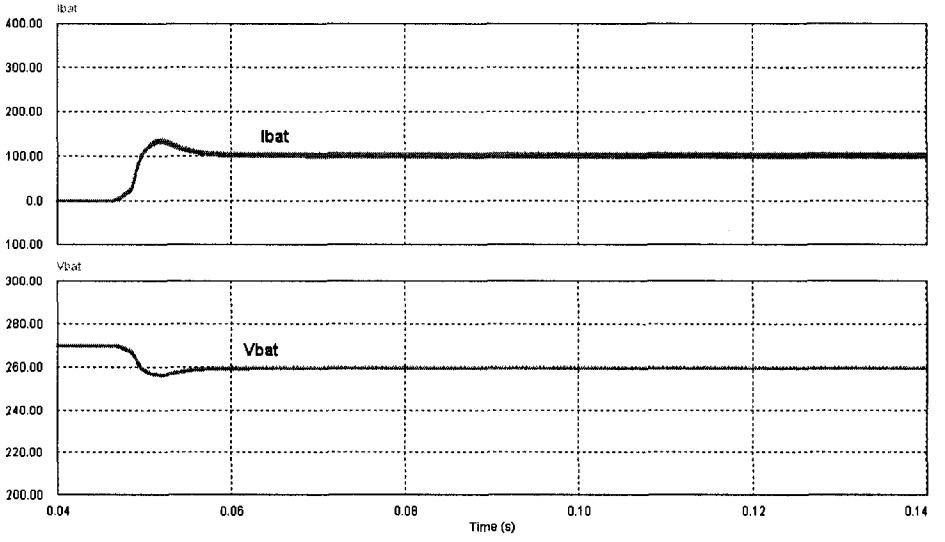

Fig. 4-18 Battery response to 26kW discharging power

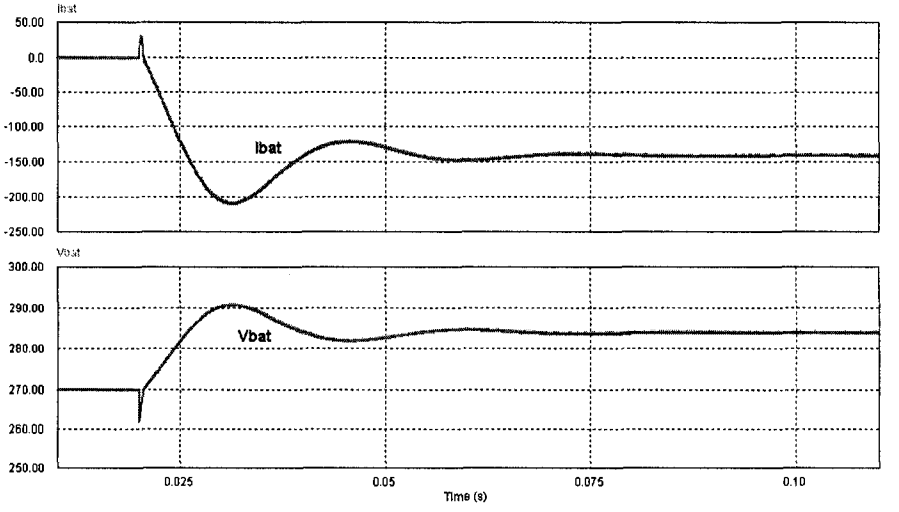

Fig. 4-19 Battery response to 40kW charging power

Further overshoot elimination and current ripple reduction can be achieved by using of anti wind-up integrator and low pass filter. Since in this topology, the fuel cell stack is directly connected to the propulsion system, regulation of fuel cell output power would not be as good as the previous topological arrangement. Therefore, the load follower control scheme is not recommended for this topology, in which fuel cell transient power fluctuation is faster and wider. The ECMS control scheme can be more suitable for this topology, where the fuel cell output is regulated, in order to provide a more constant average power demand within the high-efficiency area and the battery provides the remaining transient power.

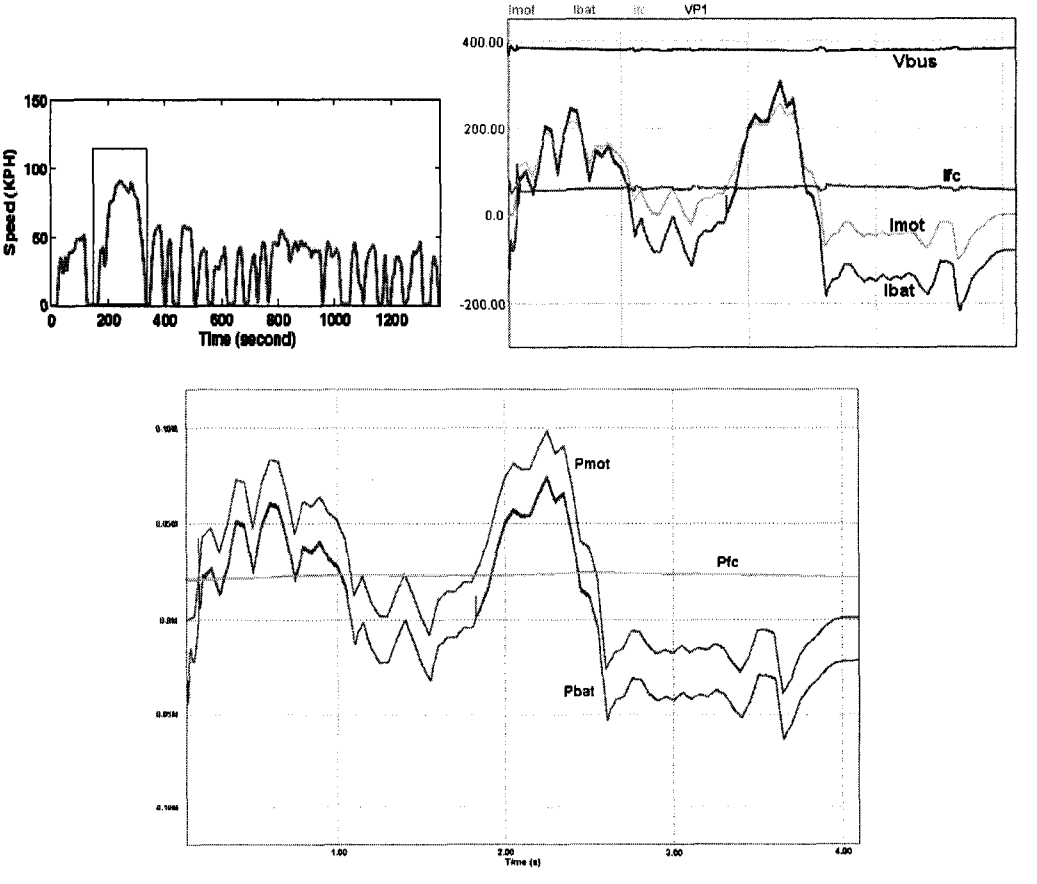

Fig. 4-20 Topology-B transient performance over a portion of the UDDS drive cycle

Fig. 4-20 illustrates the system transient performance of current and power

distributions under the ECMS scheme, during an acceleration-deceleration period, from a part of the UDDS cycle, which shows that optimal power distribution between 2 power sources can be easily implemented.

4.6 SUMMARY

This chapter dealt with the hybrid power train topology selection and power electronic control implementation, to coordinate with the supervisory power controller. Two types of power train topologies were selected for this application, based on the hybridization degree for a mid-sized hybrid SUV. It is concluded that by using topology-A (with a unidirectional DC/DC converter), interfacing the fuel cell is more suitable for mild hybridization ratios, and an interleaved boost converter is proven to a very satisfactory choice. Furthermore, using topology-B (with a bi-directional DC/DC converter), interfacing the battery is more suitable for a higher hybridization degrees, and a half bridge DC/DC converter is selected.

The power control schemes were designed for both topologies, in which the current control scheme is applied for topology-A, to directly regulate the fuel cell output power; and voltage regulation is used to regulate the fuel cell output power, by regulating the DC bus voltage and battery voltage. Simulation test results show that both control schemes can achieve power regulation according to the power command from the supervisory controller. In terms of the control strategy selection for different power train topologies, it is concluded that topology-A is more suitable for the load follower strategy, considering the flexibility for fuel cell regulation, and the ECMS is more reasonable for topology-B, from the view of fuel cell and battery protection.

CHAPTER 5

DESIGN AND FEASIBILITY STUDY OF A FUEL CELL PLUG-IN HYBRID ELECTRIC VEHICLE (FC-PHEV)

5.1 INTRODUCTION

With the ever-increasing demand for reducing emissions and improving fuel economy, the automotive industry's interest in developing alternative power-train technologies has increased dramatically. Plug-in hybrid electric vehicles (PHEVs) are gaining rapid popularity, since they represent an important technical step towards increased fuel efficiency, decreased emissions, and greater energy independence. At the same time, the limitations of battery technology, including size and weight issues, as well as short life spans, due to large number of deep charging and discharging cycles, still prove to be the major hurdle in deployment of HEVs. Besides, the use of an internal combustion engine (ICE) on board an HEV still generates green house gas emissions and limits the overall vehicle efficiency. At the same time, with the fast development of fuel cell technology, fuel cell hybrid electric vehicles (FC-HEVs) have received much attention in order to achieve high fuel efficiency and zero emissions. However, issues such as high cost, hydrogen storage, fuel reforming, and overall infrastructure are still major hurdles for FC-HEV commercialization.

Based on this background, an attractive option in the form of a plug-in fuel cell hybrid vehicle (FC-PHEV) is presented in this chapter. The FC-PHEV is proposed for a mid-sized family sedan, suitable for commuter routes. The drive train is powered by a

proton exchange membrane (PEM) regenerative fuel cell, combined with a Ni-MH battery pack. The FC-PHEV can draw electricity either from the grid or a personal eco-system, taking advantage of renewable resources like wind and solar power. Such an FC-PHEV power train arrangement presents numerous advantages, including:

- Much extended driving range without the weight penalty of batteries. Furthermore, fuel cell operation in this arrangement yields higher efficiencies. The fuel cell can be greatly downsized, and thereby, cost can be greatly reduced compared to typical FC-HEVs.
- No emissions and noise pollution. Both the battery and fuel cell system can be charged by grid electricity. Sustainability and good flexibility can be achieved by taking advantage of more efficient and low-cost off-peak power, by using renewable energy systems.
- Elimination of reliance on petroleum fuels and IC engines; much less dependence on hydrogen infrastructure.

In this chapter, the power train configuration as well as the power management problem for the proposed FC-PHEV is studied. Thereafter, the characteristics of a regenerative fuel cell and market applications will be introduced. Furthermore, the power train configuration and power component sizing of the proposed FC-PHEV will be presented. An appropriate power management strategy is designed and a complete drive train performance analysis is presented based on simulation tests. Practical issues such as cost and efficiency will also be discussed.

5.2 REGENERATIVE FUEL CELL SYSTEM

Related literature states that intensive research programs are in place for regenerative fuel cell (RFC) development, and that RFC system applications are going to be commercially viable in vehicular and aerospace markets [26]-[31]. An RFC is a device that can operate both as an electrolyzer and a typical fuel cell [28]. Recent developments in PEM fuel cell technology and electrolyzer technology make RFCs very promising alternatives to batteries for storage of energy, especially if used in conjunction with photovoltaic (PV) systems. A typical PEM based RFC is illustrated in Fig. 5-1. Such a system generally consists of a PEM electrolyzer, high-pressure hydrogen, and oxygen storage tanks, as well as the PEM fuel cell.

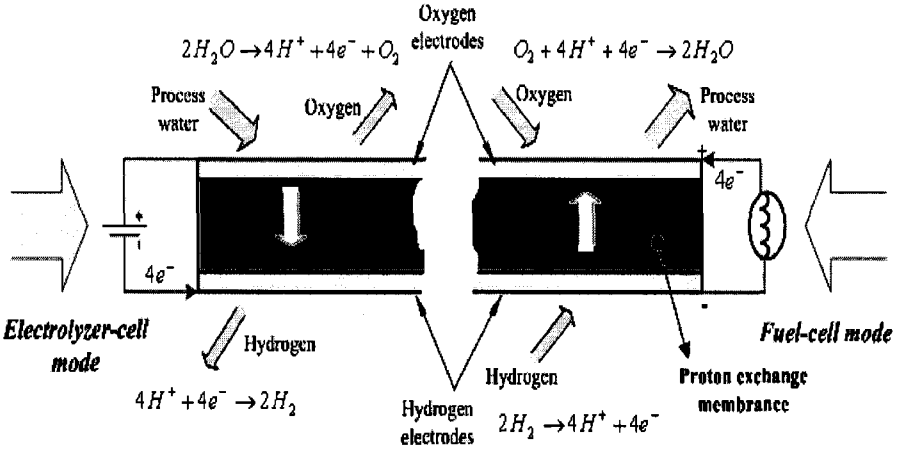

Fig. 5-1 Operation of a PEM regenerative fuel cell

In the fuel cell mode, the PEM fuel cell combines oxygen and hydrogen to produce electricity and water, whereas in the electrolysis mode, electricity and water are combined to generate oxygen and hydrogen. Therefore, this system can operate in a closed water loop. The only required input is energy, to drive the electrolyzer. As is clear, the water and the gases cycle in a closed loop with zero emissions. Such closed-system RFCs

indicate great advantages over open-system fuel cells, because pure hydrogen and oxygen are used here, which not only increase specific power output but also fuel cell efficiency, and thereby, the overall life. There also exists an obvious weight advantage for such a kind of utilized RFC. The use of a compressor can also be avoided, due to the pressurized electrolyzer [28]. PEM fuel cells operating at pressures of up to 1.0MPa have been demonstrated, and PEM electrolyzers operating at pressures up to 41MPa have also been presented in literature [30].

Table 5-1 Projected costs of PEM fuel cell and PEM-RFC

FC cost / Year	1kW PEM fuel cell (with pure H2,O2)	1kW RFC System
2004	$1100	$1700
2008	$800	$1400
2010	$600	$1100
2012	$400	$700
2016	$200	$400

Projected RFC costs are provided in Table 5-1 [26]-[28]. RFC costs are projected to be 35% greater by the year 2010 than the cost of a PEM fuel cell of the same size. While RFCs cost more than batteries on a power output basis, they are expected to be comparatively less costly than batteries on an energy-storage basis. The gas storage for RFC is estimated to be $10/kWh, for tanks smaller than 40 gallons, while for Ni-MH batteries, the cost is about $400/kWh, according to [26]. Thus, this scenario means that the combination of battery systems to provide power output, and fuel cell systems to extend range, prove to be more cost effective, than the use of either alone. This approach is particularly attractive, since such a process can be directly refueled by grid electricity, similar to plug-in batteries (usually taking advantage of solar energy and/or wind energy),

rather than relying on a hydrogen-refueling infrastructure, which makes the overall application more feasible and economical.

5.3 POWER TRAIN CONFIGURATION AND SIZING

The proposed power train configuration of the FC-PHEV is illustrated in Fig. 5-2. Both the battery and fuel cell system provide power to the motor system and either can be charged by grid electricity. In some cases, ultra-capacitors can also be used in conjunction with the battery, to further improve the vehicle dynamic performance.

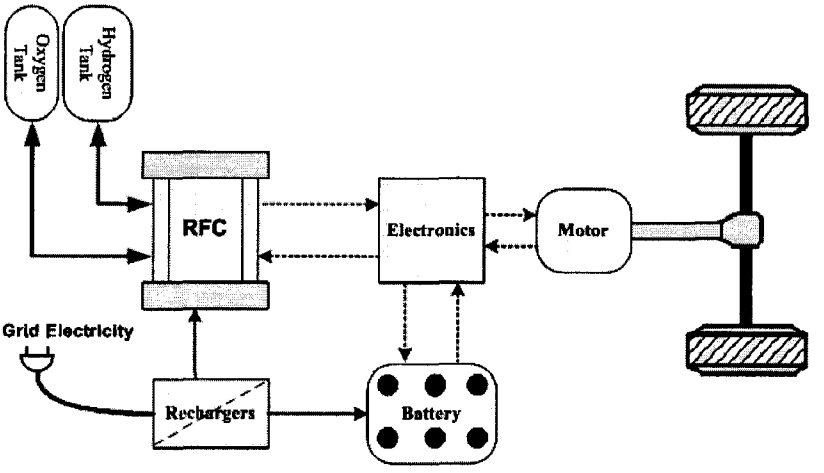

Fig. 5-2 Operation of a PEM regenerative fuel cell

The power component selection and sizing are based on the driving requirements of a mid-size family sedan. It should provide 80 miles plug-in driving range, and practical issues include component efficiency, cost, and weight. Ni-MH batteries are selected due to their high power density and long life span. The family sedan is designed for commuter type routes, which depicts limited daily driving range and limited cargo carrying capacity. Two standard driving scenarios, the Urban Dynamometer Driving Schedule (UDDS) and the Highway Fuel Economy Test (HWFET) cycle, are used for

testing under urban and highway driving conditions. The peak power for the selected driving conditions, and considering vehicle acceleration and gradeability requirements for a mid-size car, is computed to be 70kW, and the average power demand is about 30kW. Thereby, the selected motor system is a 75kW AC induction motor. The vehicle specifications and power component sizes are listed in Tables 5-2 and 5-3, respectively.

Table 5-2 Power component description

Power Components	Size and Description
RFC system	PEM fuel cell with PEM electrolyzer Rated Power: 8 kW Weight: 81kg
Battery system	Ovonic45Ah nickel metal hydride battery. No. of modules: 20 Peak power: 66kW Weight: 168kg
Motor System	75kW AC Induction motor Weight: 91kg Peak Efficiency: 0.92

Table 5-3 Vehicle specifications

Vehicle Type	Medium-size Family Sedan
HEV glider mass	636 kg
Cargo and passenger Mass	136 kg
Total Vehicle Mass	1257 kg
Frontal Area	$2.0m^2$
Coefficient of Drag	0.35

5.4 CONTROL STRATEGY DESIGN AND PERFORMANCE STUDY

5.4.1 POWER CONTROL STRATEGY DESIGN

The overall power management strategy plays a vital role in HEVs, to meet the power requirement from the traction motor, while optimizing the overall drive train

efficiency and vehicle fuel economy. A suitable real time power management strategy is designed for the proposed FC-PHEV, taking into consideration both the driving pattern as well as component efficiency. Driving conditions play an important role in power management strategy design. For urban driving cycle or long term driving conditions, the charge sustaining mode is selected, which maintains the battery state of charge (SOC) around the target value (0.6 in this case). For highway driving or short term driving conditions, the vehicle will operate in the charge depleting mode, wherein the SOC threshold is set to be minimum 0.3 and maximum 0.9. The charge depleting mode will also be used during the start up, after the battery has been fully charged, until the battery reaches the target SOC level. The driving modes can be chosen by the driver at the start of the route.

For power distribution during driving, the equivalent consumption minimization strategy (ECMS), introduced in chapter 3, is used to optimize the fuel economy. A reasonable fuel cell operating area and electrolysis charging range can be determined by a practical efficiency map, as shown in Fig. 5-3 [28].

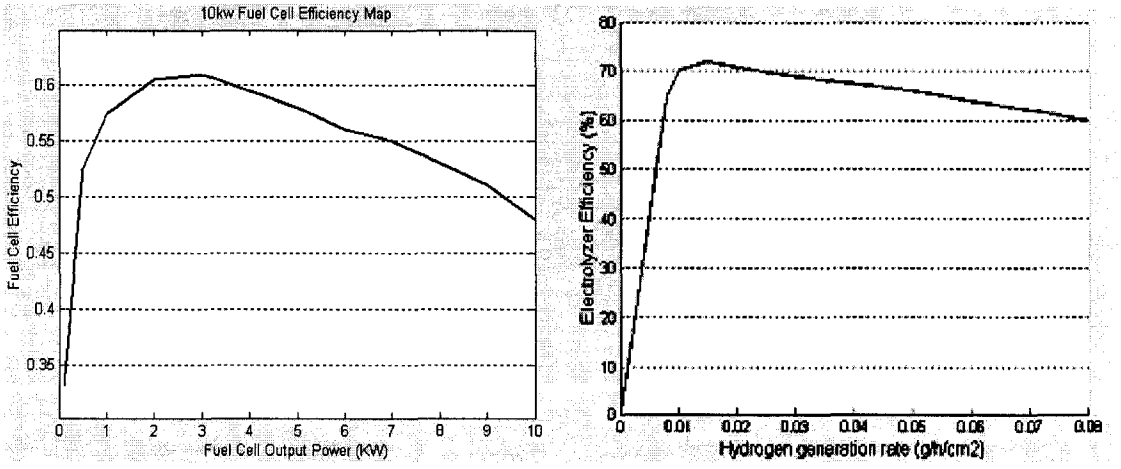

Fig. 5-3 RFC system and electrolyzer efficiency maps

Most of the time, the fuel cell operates around the high efficiency area, to provide an average power to the motor system. The fuel cell will continue to operate as long as the battery is less than fully charged. At the same time, the battery provides the remaining power, depending on the power demand, and receives regenerative braking power from the motor system. Therefore, for a typical day, after the overnight off-peak charging of battery and fuel cell, the FC-PHEV will first operate in the charge depleting mode (pure electric) as start up, until the battery SOC decreases to the target level (0.6 in this case). Thereafter, for urban driving conditions or long term driving requirements, the vehicle will work in charge sustaining mode, under the ECMS power control strategy. For highway driving conditions or very short term trips, the vehicle will work in the charge depleting mode. Thus, the fuel cell operates both as a battery charger as well as a power assist device.

5.4.2 Simulation Results and Performance Analysis

Modeling and simulation of the FC-PHEV is conducted in the Advanced Vehicle Simulator (ADVISOR) software. However, the electrolyzer part of regenerative fuel cell is not included in the model since it is difficult to get the accurate modeling data for electrolyzer mode. The overall controller performance is focused upon, wherein only the fuel cell output characteristics are considered.

After being fully charged by grid electricity during the night time, the vehicle starts up in the charge depleting mode, until the battery SOC is reduced to the target level (around 0.6). As shown in Fig. 5-4, in urban driving condition (UDDS), the FC-PHEV can drive more than 15 miles by using only the battery source.

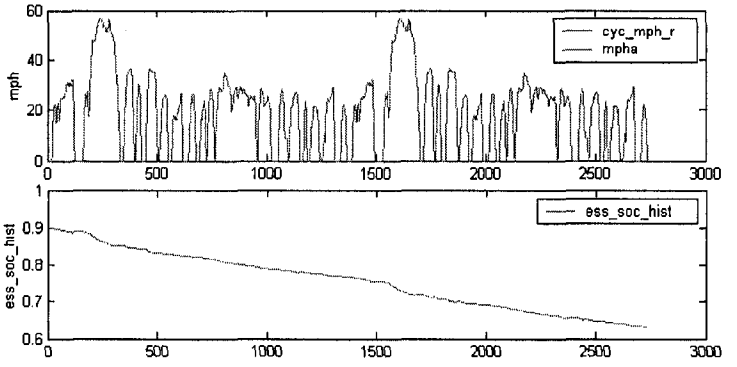

Fig. 5-4 FC-PHEV start-up in charge depleting mode

After the battery SOC recovers to the target level, the vehicle operates in the charge sustaining mode, wherein the battery SOC is maintained around target level, assisted by the fuel cell system. Fig. 5-5 illustrates the vehicle operation in 5 consecutive UDDS driving cycles. As is clear, the SOC can be controlled around 0.58, which can be independent of the driving range (the plug-in driving range under UDDS, for charge sustaining mode, is tested to be more than 80 miles, with a fuel consumption at about 460g). The fuel cell output power profile during this period is shown in Fig. 5-6.

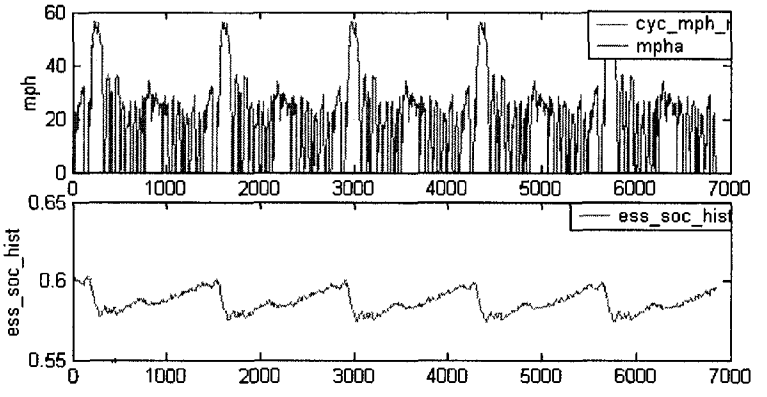

Fig. 5-5 Battery SOC profile for 5 UDDS cycles

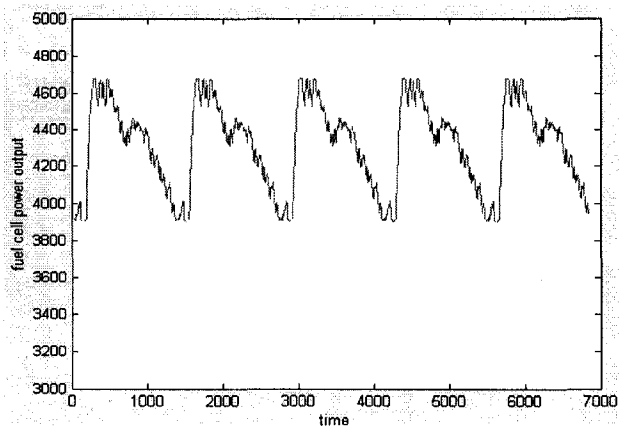

Fig. 5-6 Fuel cell power output profile during 5 UDDS cycles

Under highway driving conditions, as shown in Fig. 5-7, the vehicle operates in the charge depleting mode, since much less regenerative braking energy can be absorbed. But during this period, the fuel cell also provides assisted power to the battery, within its high efficiency range, as shown in Fig. 5-8. This plug-in highway driving range can reach over 35 miles, till the battery SOC reduces to the threshold level of 0.3. The vehicle can be charged by grid electricity after the trip ends.

Since the FC-PHEV is designed for a mid-size family sedan, which is used mainly as a commuter vehicle, a daily suburban household return cycle is studied, as shown in Fig. 5-9. The drive cycle is represented by the combination of 2 UDDS and 2 HWFET cycles. The middle zone is the charge sustaining driving zone, and the final battery SOC is set at 0.5. The total driving range is about 36 miles, and the total H_2 consumption is about 270g (A 35L automotive hydrogen tank, at 34.5MPa, can be used to store 500g H_2 in the FC-PHEV). The vehicle dynamic drivability is checked through acceleration and gradability tests, as detailed in Table 5-3, wherein all the performance criteria can meet the dynamic requirement for a mid-size sedan.

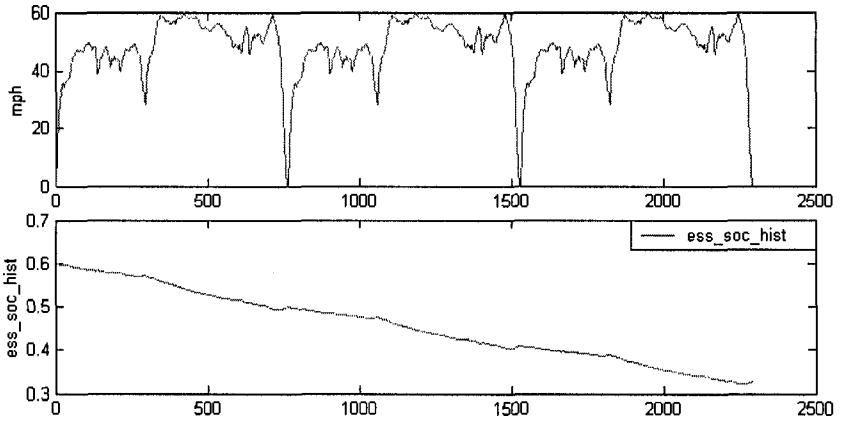

Fig. 5-7 Battery SOC profile for 3 HWFET cycles

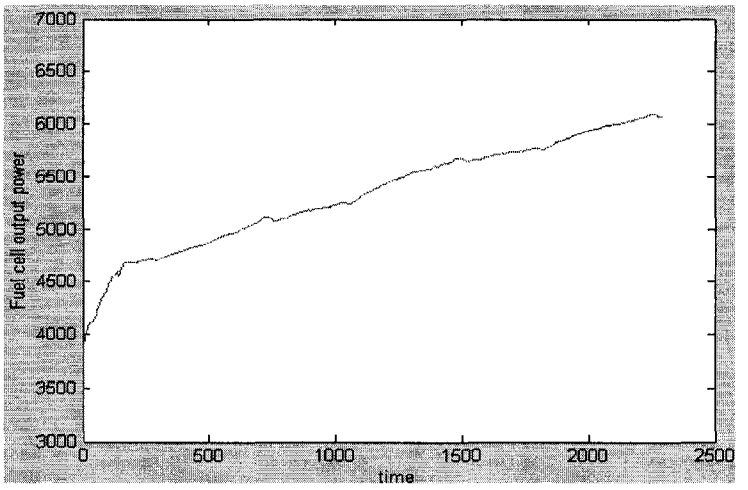

Fig. 5-8 Fuel cell power output profile during 3 HWFET cycles

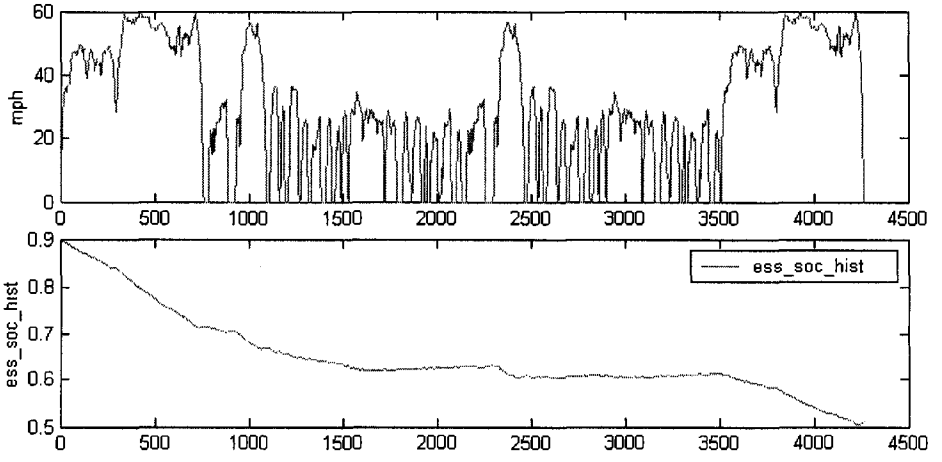

Fig. 5-9 SOC profile for a daily drive cycle

Table 5-4 Vehicle dynamic performance

Item		Result
Acceleration Time (s)	0~60 mph	8.8
	40~60 mph	4.5
	0~85 mph	19.4
Maximum acceleration (m/s^2)		4.86
Maximum speed (mph)		99.6
Gradeability (at 55mph, 20s)		20.5%

5.4.3 EFFICIENCY AND COST ANALYSIS

The complete efficiency analysis for a FC-PHEV can be very complicated, since multiple factors need to be taken into consideration, such as impact of greenhouse emissions, the efficiency of the electrical power grid, and cost-related issues. The well-to-wheels (WTW) efficiency of a FC-PHEV comprises of: grid electricity (53%), electrolysis (72%), fuel cell (55%), battery charging and discharging efficiency (96%), and the power control circuit and motor system (80%). Thus, the combined WTW efficiency of the FC-PHEV system turns out to be merely 14% efficient. In contrast, for conventional gasoline ICE vehicle, the WTW efficiency is about 15%, and for the more efficient diesel ICE, the efficiency can reach up to 22% [29]. The WTW efficiency does not seem comparable with the best ICE option. However, it does not take into account the increasing flexibility of off-peak electrical power generation using wind, solar, and nuclear energy, and the emission elimination from the plug-in fuel cell hybrid.

Table 5-5 gives an estimation of the power system cost of different advanced vehicle options. The cost of power components is projected for the year 2010. The driving range for all power train options is set at 80 miles. The electrolyzer cost is

estimated to be 25 percent of the fuel cell cost [29], and the batteries used are nickel-metal hydride (Ni-MH). As is clear, the proposed FC-PHEV is expected to be much cost effective than a pure battery electric vehicle (BEV) or a fuel cell-HEV. If the PEM fuel cells are used with air, the cost would double to $1000/kW, compared to using pure O_2. The cost of a conventional plug-in hybrid vehicle (PHEV) still seems lower than the FC-PHEV. But, at the same time, the negative effect of petroleum consumption and the emission problems of PHEVs have not been considered. Besides, the power train configuration of a FC-PHEV will be simpler than that of PHEV, due to its all-electric nature.

Table 5-6 Power train system cost comparison for different vehicle types

Options / Items	BEV	FC-HEV (O_2)	FC-PHEV	PHEV
ICE	0	0	0	$1500
PEM-FC ($500/kW)	0	$25000 (50kW)	$4000 (8kW)	0
Electrolyzer (25% *FC)	0	0	$1000	0
Battery ($400/kWh)	$18000	$3600	$4800	$6000
Total power System cost	$18000	$28600	$9800	$7500

5.5 SUMMARY

This chapter proposed a fuel cell plug-in hybrid electric vehicle (FC-PHEV) configuration, powered by combining an on-board regenerative fuel cell (RFC) and down-sized Ni-MH batteries. Such a power train option presents several attractive advantages, such as independence from H_2 refueling infrastructure or petroleum use,

elimination of green-house gas emissions and noise, allowing flexible usage of renewable energy sources and off-peak grid electricity, and the cost and weight advantages over EVs and FC-HEVs. In some cases, the FC-PHEV can also be potentially used as an emergency power supply to a house or a small office.

Furthermore, an optimal FC-PHEV supervisory power management strategy has been introduced considering the driving pattern, fuel economy, and component efficiency. The control performance and vehicle drivability are studied based on the simulation results, which show that the vehicle can achieve good drivability and enough driving range as a mid-size family sedan. The efficiency and cost factors are also comparatively discussed. Although the well-to-wheels efficiency analysis shows little advantage, the potential of charging from renewable energy sources provides a comparatively efficient option. The cost comparison indicates that the FC-PHEV can be a far better alternative, compared to a typical FC-HEV. The FC-PHEV will become more attractive with the fast development of fuel cell electrolysis technology and the decreasing trend of fuel cell cost.

CHAPTER 6

CONCLUSIONS

5.1 SUMMARY

The main objective of this thesis was to investigate the power train configuration and power management problem for fuel cell-hybrid electric vehicles (FC-HEVs). Hybridization of a fuel cell vehicle with an energy storage system increases the system efficiency, improves system dynamic performance, and reduces cost. Therefore, an appropriate hybrid power control strategy needs to be designed, in order to improve the fuel economy, component efficiency, and overall vehicle performance. An appropriate selection of control strategy needs to be taken into consideration, in order to achieve superior performance, simplicity, and feasibility of implementation and applicability to a particular hybrid power train.

The overall vehicle and is modeled and simulated in the Advanced Vehicle SimulatOR (ADVISOR) software, based on Simulink. Two types of power control strategies are optimally designed, modeled, and tested, to study their control performance. The first is the load follower scheme, which is a rule-based strategy, and the other is the energy consumption minimization strategy (ECMS), which is a cost-function based control strategy. Both control strategies are tested to be able to fulfill the vehicle performance requirements, while maintaining superior power component operating efficiency. The advantage of the load follower scheme lies in its better dynamic performance, compared to the ECMS. In addition, the load follower scheme provides a

robust, comprehensible, and uncomplicated method to create an acceptable design within a short time. A major disadvantage, though, is that it does not embody a fuel consumption optimization policy. On the other hand, the ECMS achieves optimized fuel economy and fuel cell system efficiency, while globally maintaining the battery SOC. It can shift many operating points towards the higher efficiency area, and the peak power command significantly reduces. A minor disadvantage of the ECMS usage is that some vehicle performance is sacrificed to achieve better fuel economy from the acceleration and gradability tests compared the load follower scheme. Besides, the control performance also seems sensitive to some model parameters. Thus, the accuracy of the model formulation is crucial to control performance.

In order to execute the power commands from the supervisory control strategy, it is essential to have a suitably designed power electronic system. A high power DC/DC power converter plays a vital role in the hybrid system, to regulate the power output and interface the power components to the high-voltage propulsion system. Two types of power train topologies are studied, based on the position of the converter, and are selected after considering the vehicle hybridization degree requirement. Both unidirectional as well as bi-directional converters are selected after considering component sizes, reliability, and costs. Power electronic control schemes are respectively designed for 2 power train topologies. Circuit simulation results show that the power converter controller can accurately follow the power demand from the supervisory controller, in order to achieve power conversion and distribution.

Finally, based on the background study of recent fuel cell technology, market trends, and renewable energy development, an attractive option in the form of a plug-in

fuel cell hybrid vehicle (FC-PHEV) is presented, mainly for city commuter vehicle applications, as a transition from regular FCVs. The proposed drive train is powered by a proton exchange membrane (PEM) regenerative fuel cell (RFC), combined with a Ni-MH battery pack. Both the regenerative fuel cell and the battery pack can draw electricity either from the grid or a personal eco-system, taking advantage of renewable resources. Both the fuel cell and battery can be greatly downsized and dependence on hydrogen infrastructure is much less compared to a FC-HEV. Such a FC-PHEV indicates enormous potential for short term commercialization. A suitable power control strategy was designed, with focus placed on fuel economy, component efficiency, and driving pattern. The test results show that the FC-PHEV can achieve good drivability and sufficient driving range for a typical mid-size family sedan application.

5.2 SUGGESTIONS FOR FUTURE WORK

(1) Hardware-in-the-loop implementation and study of a scaled-down prototype power train system and power controller for FC-HEV, using dSPACE.

(2) Development of an energy storage system that combines high power-density ultra-capacitors and a high energy-density battery pack, in order to further improve the dynamic performance and drive train efficiency.

(3) Design of an optimal power control strategy, to manage the power distribution between the fuel cell stack, battery pack, and ultra-capacitor bank.

REFERENCES

[1] R. D. Strattan, "The electrifying future of the hybrid automobile," *IEEE Potentials*, vol. 23, no. 3, pp. 4-7, Aug. 2004.

[2] K. T. Chau and Y. S. Wong, "Overview of power management in hybrid electric vehicles," *Energy Conversion and Management*, vol. 43, no. 15, pp. 1953-1968, Oct. 2002.

[3] C. C. Chan, "The state of the art of electric, hybrid, and fuel cell vehicles," *Proceedings of the IEEE*, vol. 95, no. 4, pp. 704-718, April 2007.

[4] M. Ferdowsi, "Plug-in hybrid vehicles - A vision for the future," in Proc. *IEEE Vehicle Power and Propulsion Conf.*, Arlington, TX, Sept. 2007, pp. 457-462.

[5] J. H. Hirschenhofer, D. B. Stauffer, R. R. Engleman, and M. G. Klett, "Fuel Cell Handbook," 4th Edition, DOE/FETC-99/1076.

[6] K. Johansson and P. Alvfors, "Steady-state model of a proton exchange membrane fuel cell system for automotive applications," in Proc. *International Conf. on Efficiency, Costs, Optimization, Simulation, and Environmental Aspects of Energy and Process Systems*, Enschede, The Netherlands, July 2000, pp. 725–736.

[7] US DOE, *Energy Efficiency and Renewable Energy*, Jan. 2008, see: http://www.eere.energy.gov/hydrogenandfuelcells/fuelcells/fc_types.html

[8] National Renewable Energy Laboratory, "Advanced Vehicle Simulator (ADVISOR) Documentation," see http://www.ctts.nrel.gov/analysis/advisor_doc

[9] T. Markel, A. Brooker, T. Hendricks, V. Johnson, K. Kelly, "ADVISOR: a systems analysis tool for advanced vehicle modeling," *Journal of Power Sources*, vol. 110, no. 2, pp. 255-266, Aug. 2002.

[10] D. D. Boettner and M. J. Moran, "Proton exchange membrane (PEM) fuel cell-powered vehicle performance using direct-hydrogen fueling and on-board methanol reforming," *Energy*, vol. 29, no. 12-15, pp. 2317-2330, Oct. 2004.

[11] J. Park, B. Raju, and A. Emadi, "Effects of An ultra-capacitor and battery energy storage system in a hybrid electric vehicle," *Society of Automotive Engineers (SAE) Journal,* Paper No. 2005-01-3452, 2005; and, in *Proc. SAE 2005 Future Transportation Technology Conference*, Chicago, IL, Sept. 2005.

[12] V. H. Johnson, "Battery-performance models in ADVISOR," *Journal of Power Sources*, vol. 110, no. 2, pp. 321-329, Aug. 2002.

[13] A. P. Roussean, R. Ahluwalia, and Q. Zhang, "Energy storage requirements for fuel cell vehicles," in Proc. *SAE World Congress*, Detroit, MI, March 2004, Paper No. 2004-01-1302.

[14] H. Y. Cho, W. Gao, and H. Ginn, "A new power control strategy for hybrid fuel cell vehicles," in Proc. *IEEE Workshop on Power Electronics in Transportation*, Detroit, MI, Oct. 2004, pp. 159-166.

[15] C. Liang and W. Qingnian, "Energy management strategy and parametric design for fuel cell family sedan," in Proc. *SAE Future Transportation Technology Conf. and Expo.*, Costa Mesa, CA, Aug. 2001, Paper No. 2001-01-2506.

[16] H. S. Ahn and N. S. Lee, "Power distribution control law for FCHEV-A fuzzy logic-based approach," in Proc. *IEEE International Conf. on Control and Automation*, Budapest, Hungary, June 2005, pp. 486-490.

[17] N. S. Lee, G. M. Jeong, and H. S. Ahn, "Improvement of fuel economy using fuzzy logic-based power distribution control strategy for a FCHEV," in Proc. *IEEE*

International Conf. on Computational Intelligence and Security, Guangzhou, China, Nov. 2006, vol. 1, pp. 891-894.

[18] J. S. Lai and D. J. Nelson, "Energy management power converters in hybrid electric and fuel cell vehicles," *Proceedings of the IEEE*, vol. 95, no.4, pp. 766-777, April 2007.

[19] G. Paganelli, Y. Guezennec, and G. Rizzoni, "Optimizing control strategy for hybrid fuel cell vehicles," in Proc. *SAE International Congress*, Detroit, MI, March 2002, Paper No. 2002-01-0102.

[20] P. Rodatz, G. Paganelli, A. Sciarretta, and L. Guzzella, "Optimal power management of an experimental fuel cell/supercapacitor-powered hybrid vehicle," *Journal of Control Engineering Practice*, vol. 13, no. 1, pp. 41-53, Jan. 2005.

[21] J. Liu and H. Peng, "Control optimization for a power-split hybrid vehicle," in Proc. *IEEE American Control Conf.*, Minneapolis, MN, June 2006, pp. 14-16.

[22] A. Schell, H. Peng, D. Tran, E. Stamos, and C. C. Lin, "Modeling and control strategy development for fuel cell electric vehicles," *Annual Reviews in Control*, vol. 29, pp. 159-168, 2005.

[23] K. Rajashekara, "Power conversion and control strategies for fuel cell vehicles," in Proc. *29th Annual Conf. of the IEEE Industrial Electronics Society*, Roanoke, VA, Nov. 2003, vol. 3, pp. 2865-2870.

[24] X. Huang, T. Nergaard, J. S. Lai, X. Xu, and L. Zhu, "A DSP based controller for high-power interleaved boost converters," in Proc. *IEEE Applied Power Electronics Conf. and Expo.*, Miami, FL, Feb. 2003, pp. 327-333.

[25] C. Liu, T. Nergaard, L. Leslie, J. Ferrell, X. Huang, T. Shearer, J. Reichl, J. Lai, and J. Bates, "Power balance control and voltage conditioning for fuel cell converter with multiple sources," in Proc. *IEEE Power Electronics Specialists Conf.*, Cairns, Australia, vol. 4, pp. 2001-2006.

[26] G. J. Suppes, "Plug-in hybrid with fuel cell battery charger," *International Journal of Hydrogen Energy*, vol. 30, no. 2, pp. 113-121, Feb. 2005.

[27] G. J. Suppes, "Plug-in HEV roadmap to hydrogen economy," *SAE Transactions*, vol. 114, no. 3, pp. 1705-1713, Paper No. 2005-01-3830, 2005.

[28] F. Barbir, T. Molter, and L. Dalton, "Regenerative fuel cell for energy storage: efficiency and weight trade-offs," *IEEE Aerospace and Electronics Systems Magazine*, vol. 20, no. 5, pp. 35-40, March 2005.

[29] G. J. Suppes, S. Lopes, and C. W. Chiu, "Plug-in fuel cell hybrids as transition technology to hydrogen infrastructure," *International Journal of Hydrogen Energy*, vol. 29, no. 4, pp. 369-374, March 2004.

[30] A. Leonida, F. Militsky, B. Myers, A. H. Weisberg, "Applications and development of high pressure PEM systems," in Proc. *Portable Fuel Cells Conf.*, Lucerne, Switzerland, June 1999, pp. 253-268.

[31] D. J. Bents, V. J. Scullin, B. J. Chang, D. W. Johnson, C. P. Garcia, and I. J. Jakupca, "Hydrogen-oxygen PEM regenerative fuel cell development at the NASA Glenn Research Center," see: http://gltrs.grc.nasa.gov/reports/

[32] D. Wu and S. S. Williamson, "Status review of power control strategies for fuel cell based hybrid electric vehicles," in Proc. *IEEE Electrical Power Conf.*, Montreal, Canada, Oct. 2007, pp. 218-223.

[33] D. Wu and S. S. Williamson, "Performance characterization and comparison of power control strategies for fuel cell based hybrid electric vehicles," in Proc. *IEEE Vehicle Power and Propulsion Conf.*, Arlington, TX, Sept. 2007, pp. 55-61.

[34] D. Wu and S. S. Williamson, "A novel design and feasibility analysis of a fuel cell plug-in hybrid electric vehicle," in Proc. *IEEE Vehicle Power and Propulsion Conf.*, Harbin, China, Sept. 2008.